Carbon-bearing Grains of Asteroids to Form Organic Life Systems on Active Water-Planet Earth

Yasunori MIURA

Department of Earth System Sciences, Faculty of Science, Yamaguchi University

Introduction: The major two groups of inorganic and organic compounds on active water-planet Earth are originated as two Silicon (Si)-bearing groups and Carbon (C)-bearing groups at primordial stages on the Solar System. From light elements are actively existed on upper systems of air and liquid phases, though heavier elements are mainly situated in lower solid to fluid phases stable at lower PT conditions relatively. Therefore, Carbon -bearing organic life activity mainly existed surface of rocky grounds, which are high-level life systems ate the similar of three phases of the earth with three system layered structure which are the same of Earth-related structure fundamentally. Therefore, we discuss high-level life species in active-water Earth as special planet production relatively, though all elements and solids states recently formed. The purpose to show the more detail consideration carbon-related grains and life-related concept here [1-6].

Carbon significance: Ions and elements (isotopes) are formed chemically in the star (nuclear reaction, as in the Sun) condition, which can find widely in the space world. However rock and mineral (crystal) with carbon contents are formed by giant atomic composition and structure (at more stable reaction time and space) which are found on the surface on rocky body of Asteroids or planets (as in Earth-type planet and Asteroids). This means that carbon-bearing grains which are similar structure process of the rock of the Earth with stable low PT conditions as longer existences on the Solar System [1-4].

Energy sources significances: The present energy sources on the Active Earth are three sources of planetary impacts (or meteorite impacts), Earthquake and volcano. 1) The outer-spaced sources (to the Earth) are meteorite impact, gravitational sources of Earth quake, and volcano which are occurred on active Earth. 2) Probable missing sources of meteorite- meteorite (Asteroids) impacts around Earth are considered to be occurred (especially sources of fluid waters and carbon gases on the Earth) [3-6] (Table 1).

Carbon-bearing rocks and grains variety: Grains on the Solar Systems are used mixed minerals and unclear intermediate fluids with glassy solids usually. However, terminology of organic comopound is used for prefect crystal and crystalline solids (definition on Earth organic crystals), though its crystal has been formed at stable condition with every surface on the rocks widely or longer. Therefore, crystal-like parts of organic grains on Asteroid (on the Moon and Mars also), which are different completely by Earth's organic crystal. Main difference is that Earth organics are completely crystal (with stable higher PT condition with longer condition), though Asteroid crystal-like parts are quick shock-wave condition with unstable and less time reaction with various PT conditions). It might be used organic-like or meteoritic organic grains for extraterrestrial organic grains [5-6].

Inhomogeneous rocks on the Earth: Active Earth shows phase states of air, liquid and solid uniform materials, though these systems are slow, long changes with quick mixing. Especially organic grains are remained last formation. In fact, Earth surface is formed largely sea bottom rocks of carbonates even large continents widely now which show wide sea bottom rock of carbonate rocks are as first rock. Even in the present sea bottom are remained changed shapes by ocean-impact effects mainly. It is not continuous cyclic structure of active Earth (even longer ca.4.6Ga years). This means that original Asteroid organic grains are started to many organic formation except longer high PT condition possible in active water-planet. This shows that many sea and

land rocks with organic grains are formed by various surface sites and kinds on the Earth now [6] (Table 1).

Table.1 Organic grains of the Earth, Asteroid and other extraterrestrial bodies.

Celestial bodies	Organic grains	Carbon-bearing System
Earth (active, water planet)	Perfect crystals with mixed as rocks	Organic life & inorganic bone system (3 phases as Earth)
Asteroids, the Moon & Mars	Shocked organic grains mixed solids	C-bearing, SiC-bearing & bone- solids.

Summary: The present works are summarized as follows.

1. Active planet Earth shows three phase system with variable changed and remained on the rocks with carbon-bearing and organics grains.
2. Organic grains with stable in the low PT conditions are found on Asteroids the Solar System widely.
3. The present energy sources are planetary impacts, and gravitational sources are also found in Asteroids impacts on Asteroids are occurred (as fluid sources).
4. Organic grains on the Solar Systems are used mixed and unclear intermediate fluids with glassy solids. Asteroid mineral-like parts are quick shock-wave condition as meteoritic solid rocks.
5. Earth surface remade as various active behavior, originally from Asteroid rock widely.

References: [1] Miura Y. (2018) IMA-22,1189. [2] Miura Y. (2023) JAMS. E5-15. [3] Miura Y. (1996) Shock-Wave Handbook (SV, Tokyo),1073-1209. [4] Miura Y. and Kato T. (1993) AIP, 283, 488-492. [5] Miura Y. (1992) Celestial Mechanic. & Dynamical Astro. (KA), 54, 249-253. [6] Y. Miura (2024) In this volume.

SULFUR ISOTOPIC ANOMALY IN A RYUGU SULFATE

Maitrayee Bose[1*], Robert A. Root[2], Yunbin Guan[3], Jacob Eaton[4], Axel Wittmann[5],
Thomas Skrmetti[1], Steven J. Desch[1]

[1]*School of Earth and Space Exploration, Arizona State University, Tempe, AZ 85287, USA.*
[2]*Department of Environmental Science, University of Arizona, Tucson, AZ 85721, USA.*
[3]*Division of Geological and Planetary Sciences, California Institute of Technology, Pasadena, CA 91125, USA.*
[4]*School for Engineering, Matter Transport and Energy, Arizona State University, Tempe, AZ 85287, USA.*
[5]*Eyring Materials Center, Arizona State University, Tempe, AZ 85287, USA.*

Carbonaceous chondrites (CCs) provide evidence for timing of water activity after planetesimal formation, episodic aqueous events, evolution of volatiles, and formation of secondary phases. Ryugu belonging to the CI class of CCs is a least terrestrially contaminated samples from an outer solar system asteroid. Prior to our study, Yoshimura et al. (2023) found that the salt extracts contain soluble sulfur-bearing species such as polythionic acids, alkylsulfonates, hydroxyalkylsulfonates as well as thiosulfate. Our team identified a lone sulfate grain in asteroid Ryugu particle A0070 using µXANES (Figure A) and performed sulfur isotopic analysis of the calcium sulfate grain with the NanoSIMS (Figure B). The anomalous sulfur signature is derived from irradiation of the solar system's parent molecular cloud by nearby massive stars (e.g., Vacher et al. 2021). Based on these data, we confirm that Ryugu formed much farther from the Sun, near where comets formed, and where the sun's UV light was too weak for photochemistry. I will present the published results (Bose et al. 2024) and discuss the consequences of aqueous alteration in Ryugu and the degree of lateral mixing in small bodies.

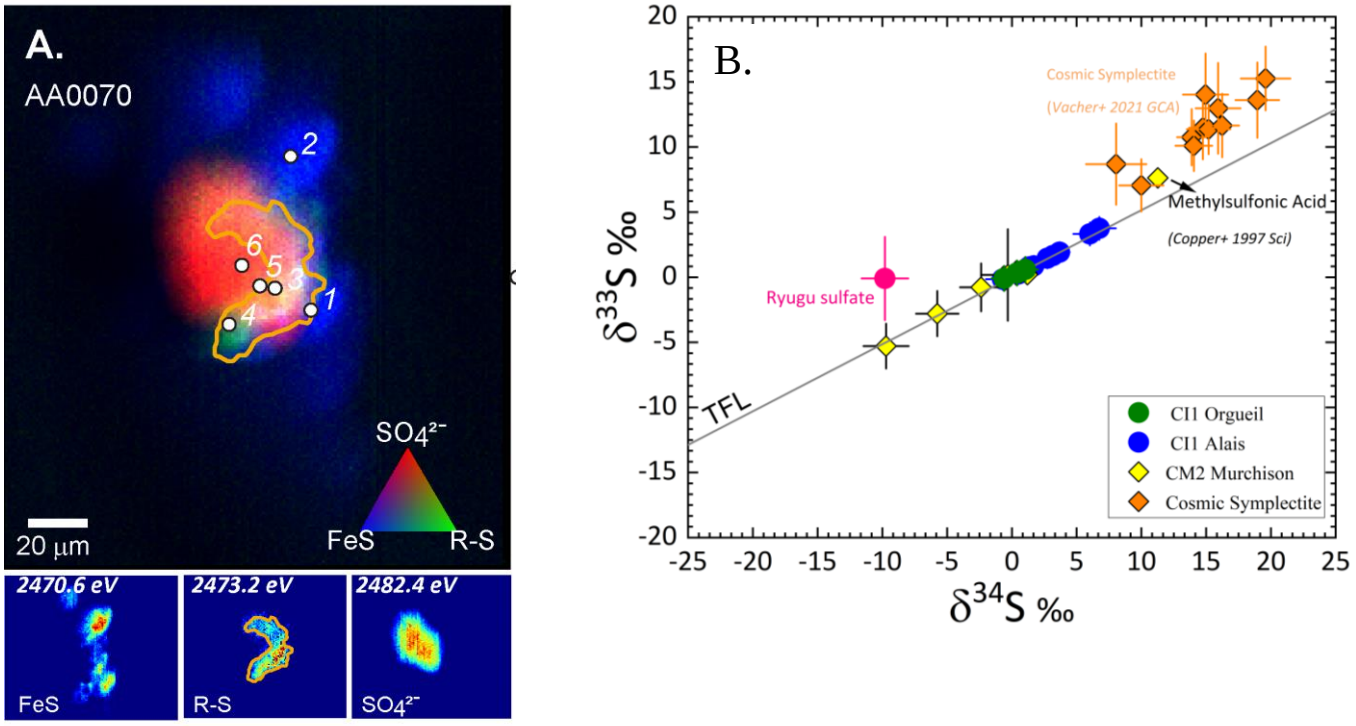

Figure (A) The thiol (in green) forms a partial rim, about 10 µm wide around a calcium sulfate grain (in red). The rim is surrounded by smaller monosulfide grains (in blue). **(B)** Three-sulfur isotope plot showing the sulfur isotopic composition of sulfides in several CC meteorites, cosmic symplecties (1), methylsulfonic acid (2), and the thiol-and sulfate-bearing composite grain identified in Ryugu particles A0070 with a $\Delta^{33}S = 5 \pm 2‰$ (1σ).

References

[1] T. Yoshimura et al. 2023. Nature Communications 14: 5284. [2] G. Vacher et al. 2021. Geochimica et Cosmochimica Acta 309: 135. [3] G. W. Cooper et al. 1997. Science 277: 1072. [4] Bose et al. 2024. Science Advances 10, eadp3037.

P, S, and K as Tracers of Aqueous Processing on Ryugu

G. J. Flynn[1], and P. Northrup[2]
[1]*SUNY-Plattsburgh, 101 Broad St., Plattsburgh, NY 12901 (flynngj@plattsburgh.edu)*
[2]*Stony Brook University, Department of Geosciences (paul.northrup@stonybrook.edu).*

JAXA's Hayabusa2 spacecraft delivered ~5.4 g of material from asteroid 162173 Ryugu. Nakamura et al. [1], who analyzed seven samples from the first collection site, indicated the major lithology was dominated by phyllosilicates, with carbonates, Fe-sulfides, Fe-oxides, and Fe-bearing hydroxyapatite. We were loaned five polished sections prepared from 3 to 5 mm size fragments from the first collection site – A0026-01, A0026-02, A0055-1, A0055-2, and A0055-3. These samples were studied previously. Tack et al. [2] measured REEs in A0055, before it was sectioned, and found REEs were mainly enriched in some Ca- and Sr-rich phases they suggested were apatite. Nakamura et al. [1] found CI-like bulk element abundance in 17 samples including A0026 and A0055. Gainsforth et al. [3] examined a FIB section from A0026. Mikouchi et al. [4] analyzed polished sections of both A0055 and A0026. The abundant phyllosilicates [1] demonstrate there was significant hydrothermal processing of these Ryugu samples. Likely products of this alteration are phosphates, carbonates, and sulfates whose abundances and compositions can characterize the fluids responsible for the alteration. To study these minerals, we used synchrotron x-ray fluorescence (XRF) to map element distributions and x-ray absorption spectroscopy (XAS) to characterize the minerals in the five sections. We focused on P, S, and K, which are sensitive indicators of aqueous mobilization.

P-mapping: Synchrotron XRF element mapping of the three A0055 sections clearly show two distinct P-lithologies (Fig. 1), with about half of each section having numerous, relatively large P-rich grains while the other half has smaller P-rich grains. The mean P/Si ratio in each lithology of the A0055 sections is quite consistent, with P/Si about 0.04 to 0.05 in the high-P areas and an order-of-magnitude lower, ~0.005, in the low-P lithology. The two A0026 samples have a more uniform distribution of P-rich grains which are smaller than the grains in the high-P lithology of the A0055 samples, but more numerous than those in the A0055 low-P lithology. The P/Si ratio in the A0026 sections is ~0.025, distinct from the high- and low-P lithologies in A0055, suggesting these Ryugu samples experienced at least three distinct degrees of hydrothermal processing.

Mikouchi et al. [3] characterized the same dry polished [1] A0055-1 section that we examined, determining the degree of aqueous processing based on the abundance and types of carbonate. In A0055-1 they found no olivine bearing clasts, present in their Lithologies I and II, which show the lowest aqueous processing. They identified three lithologies in A0055-1 based on carbonates: Lithology III dolomite-bearing; Lithology V carbonate aggregates; and Lithology VI carbonate-poor (<1 vol.%). Our XRF maps of A0055-1 show very low P in their Lithology VI areas, with P/Si ranging from 0.0048 to 0.0082. This suggests the carbonate-poor regions experienced very little deposition of P from the fluid that produced phyllosilicates. However, the low-P and high-P regions in A0055-1 both overlap their carbonate Lithology III. Our Ca-XAS and Mn-XAS of carbonates in these samples identified Mn-bearing dolomite as the dominant carbonate (Fig. 2).

Apatite: The apatite structure accepts a wide range of elements, so it is a good indicator of fluid composition. Since apatite accepts F, Cl, or OH in the anion position, the proportions of F, Cl and OH in apatite reflect the halogen and water content of the fluid. Gainsforth et al. [3] identified one apatite grain in an A0026 FIB section and found a Mn-poor core with a Mn-rich zone on the surface enriched in Fe, F, and Na compared to the core. This suggests alteration by two different fluids.

All Ca-apatite grains have distinctive P-XAS, with a peak at ~2152 eV and a shoulder on the high-energy side. The energy of this shoulder peak shifts progressively lower in energy as the apatite composition varies from fluorapatite to hydroxyapatite to chlorapatite. Most P hot-spots in these five sections have P-XAS spectra consistent with apatite (Fig. 3), which is believed to be a hydrothermal alteration phase. The small difference in position of the shoulder at ~2156 eV in the Ryugu apatite spots, compared to the fluorapatite standard (top spectrum in Fig. 3), indicates the Ryugu apatite has significant hydroxy- and/or chlorapatite components. Some of the Ryugu apatite grains showed Cl spatially coincident with the apatite in the XRF maps. To address the question of Cl in the apatite we preformed Cl-XAS, which demonstrated that the Cl was not in the apatite crystals. (Cl is present in high abundance in the epoxy mounts.) The absence of significant chlorapatite combined with the XAS spectral shift from fluorapatite indicates a significant hydroxyapatite component in the Ryugu samples. The quantitative F:OH:Cl ratio in individual apatite crystals will be determined in the planned electron microprobe analyses.

A particle-size effect on the XAS has been described in apatite XAS by Szerlag (in press). The peak height is lower in more crystalline spots due to electronic interactions across larger crystalline domains. We see significant variations in peak heights in different spots in both A0026 and A0055 that have the same P count rate, indicating that some spots are nanocrystalline aggregates or highly disordered while other spots are larger, well crystalline apatite. Seifert et al. [5], using cathodoluminescence, observed similar results in Bennu samples. They reported complex luminescence zoning in some anhedral apatite grains that range in size from about 5 to 12 μm in a Bennu sample. Our planned electron microprobe analyses should reveal if the individual apatite grains in these aggregates differ in composition, suggesting they formed from fluids of different compositions.

Although most of the P hot-spots were identified as apatite by XAS, there were two types of exceptions. A few phosphates showed no shoulder on the high energy side of the pre-edge peak (e.g., Fig. 3, bottom spectrum). Electron microprobe characterization of these phosphate spots may allow identification of this phase. In addition, we found rare, small phosphides in the matrix. The large difference in the pre-edge peaks between phosphide and phosphate in P-XAS allowed functional group specific mapping of phosphide and phosphate. Both A0055 and A0026 had regions where phosphide and phosphate were both identified (Fig. 4). However, we did not see phosphate rims surrounding phosphide cores as would be expected if an initial phosphide were attacked and incompletely altered by the fluid. Mikouchi et al. [4] identified Fe,Ni phosphide associated with

olivine [3] in grains from the second collection site. However, we found rare, small phosphides in these A0026 and A0055 sections (Fig. 3), indicating incomplete alteration of phosphide, even where Mikouchi et al. found no olivine [3].

Sulfide/Sulfate: Alteration of sulfide to sulfate has been reported in CM chondrites [6]. Sulfate is easily distinguished from sulfide because of the large energy difference in S-XAS. Sulfate is characterized by a peak at ~2483 eV, as illustrated by the bottom spectrum in Fig. 5, which also shows a sulfate standard. The upper set of spectra show 3 spots on A0026-02, all matching pyrrhotite with no sulfate, while the lower set are 4 spots on A0055-1 that also match pyrrhotite but with some sulfate within the 5-µm beam spot size. The sulfate in the A0055 sections suggests significant interaction with an oxidizing fluid. If all the sulfide grains experienced the same degree of aqueous processing, resulting in the same depth of alteration, we would expect the S hot-spots to show an anti-correlation between sulfate/sulfide ratio and size. We see no evidence for this correlation, suggesting different regions of these samples experienced different degrees of hydrothermal processing, The S/Si ratio ranges from 0.38 to 0.56, bracketing the CI ratio, in these Ryugu samples.

We identified grains of sulfide surrounding silicates (Fig. 6, left). These features may be similar to the inclusions identified in Bennu samples and Tagish Lake by Smith et al. [7]. These inclusions were described as being from 2 to 15 micrometers in size with a mostly homogeneous interior consisting primarily of fine-grained Mg-rich phyllosilicates with a rim of hexagonal sulfides. They suggested that these clasts likely formed under reducing conditions, possibly enstatite chondrite material exogenous to Bennu. We also identified circular rims of phosphate surrounding silicates, which need further study, in these Ryugu samples.

K-distribution: We mapped the K distribution, and found K to be heterogeneously distributed, but spatially coincident with the phyllosilicates. However, the low-K and high-K regions in A0055-1 (Fig. 6, right) do not correlate with any of the lithologies from Mikouchi et al. [4] or with the low-P and high-P lithologies we identified (Fig. 1). It is not clear whether this heterogeneous K distribution resulted from uneven distribution of the fluid or subsequent K leaching by the fluid.

Taken together, these results suggest the Ryugu parent body experienced multiple episodes of hydrothermal processing by fluids of different compositions. Further characterization of these Ryugu samples is in progress.

References: [1] Nakamura, T. et al. (2023) Science 379, eabn671. [2] Tack et al. (2022) Earth, Planets, Space 74, #146. [3] Gainsforth, Z. et al. (2024) Meteoritics and Planetary Science, doi: 10.1111/maps.14161. [4] Mikouchi et al. (2022) https://curation.isas.jaxa.jp/symposium/abstract/2022/S22-01. [5] Seifert et al. (2024) MetSoc, Abstract #6208. [6] Airieau et al. (2005) GCA, 69, 4166–4171. [7] Smith et al. (2024) MetSoc Abstract #6075.

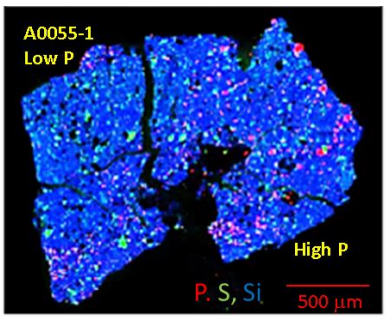

Figure 1: P, S, Si 3-color XRF map of A0055-1.

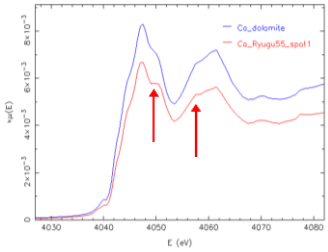

Figure 2 Ca- XAS of a large carbonate grain in A0055-1. The features that distinguish the bilayered carbonate (dolomite) from monolayered carbonates calcite or Ca-bearing magnesite are indicated by the arrows.

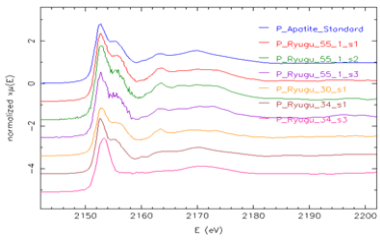

Figure 3: P-XAS of fluorapatite (top), and Ryugu P hot-spots. The bottom spectrum shows a phosphate with no shoulder on the peak.

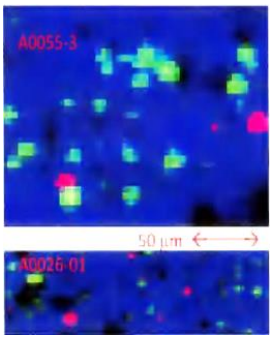

Figure 4: Phosphide (red) and phosphate (green) in A0055-3 and A0026-01.

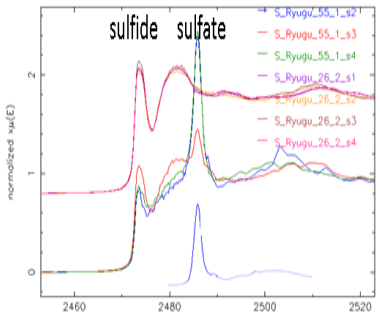

Figure 5: S-XAS of A0026-02 (top three spectra) showing only sulfide, and S-XAS of A0055-1 (next four spectra) showing sulfate as well as sulfide.

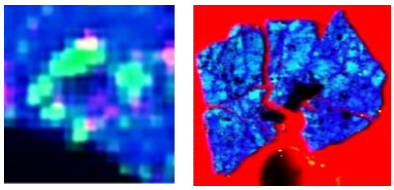

Figure 6: (Left) Three color image showing the sulfide grains (green) forming a rim around a silicate region of A0026-01. (Right) Cl (red), K (green), Si (blue) 3-color map (K shown in light blue) of A0055-1. (Cl in epoxy.)

Trace Oxygen Measurements of Asteroid Sample Storage Desiccators

M. Montoya[1], C. J. Snead[2], F.M. McCubbin[2], R. Resendez[1], F. Cantu[1], J. Ponce[1]
[1]JETS II, NASA Johnson Space Center, Houston, TX 77058, USA.
[2]NASA Johnson Space Center, Houston, TX 77058, USA.

The Astromaterials Curation facility at the NASA Johnson Space Center is currently curating more than 120 g of carbonaceous asteroid Bennu material as well as over 500 mg of asteroid Ryugu [1 and 2]. These astromaterials are stored in isolating desiccators and gloveboxes under a continuous purge of pure (<1 ppm O_2) gaseous nitrogen. The oxygen and moisture concentrations in our OSIRIS-REx sample processing gloveboxes are continuously monitored via integrated sensors; however, our sample storage desiccators lack integrated oxygen and humidity sensors. In previous studies, we used PreSens Fibox 4 trace oxygen meters and optochemical PSt9 spot sensors to measure the oxygen concentrations in candidate asteroid sample containers that had been sealed in nitrogen; we determined that Eagle stainless steel containers inhibit the ingress of external oxygen for several weeks [3]. This optochemical sensor technology allowed us to take precise, contactless measurements within a trace range of 0 to 200 ppmv O_2. The effectiveness of the trace oxygen sensors in our container experiments inspired us to utilize them to assess the performance of our desiccators that previously lacked trace oxygen monitoring.

In this study, our goal was to determine the quality of the nitrogen purge in the isolating desiccator under normal operating conditions by measuring the trace oxygen content. Utilizing optochemical sensor technology, we determined how long the oxygen concentration takes to reach an equilibrium in the desiccator; that is, determine the rate at which the oxygen diffusion into the desiccator equals the rate at which oxygen diffuses out of the desiccator via N_2 purge. Additionally, we wanted to determine the oxygen concentration at this equilibrium, the state in which our desiccators are in during normal operating conditions.

We tested a custom three chamber desiccator manufactured by Germfree using a PSt9 trace oxygen sensor spot that was mounted into a ¼" National Pipe Tapered (NPT) metal flow-through cell and attached it to the desiccator exhaust. The desiccator consists of top, middle, and bottom isolating chambers. The top chamber door was opened for several minutes to simulate a sample exchange, it was sealed, and then purged ~15 Standard Cubic Feet per Hour (SCFH). Oxygen measurements were automatically recorded via the Fibox 4 trace oxygen meter in 5-minute intervals over the course of a 24-hour period.

Our results indicate the desiccator reached an equilibrium value of 10-15 ppm O_2 after ~5 hours (Fig. 1). This data allows us to explore standards for purging and exchange protocols that can be applied to similar types of desiccators in Hayabusa2, OSIRIS-REx, and for sample return collections. The assessment of the internal gaseous compositions of desiccators also allows us to share with the community the N_2 environment in which many of our asteroid samples and hardware are securely curated. Future measurements will include other nitrogen flow rates and measuring the trace oxygen concentration as a function of time for the levels of the previous commercial desiccator in which the Hayabusa2 sample collection was stored. We will also analyze how long the desiccators hold N_2 after being disconnected from their N_2 source, an extended measurement for sample security reassurance.

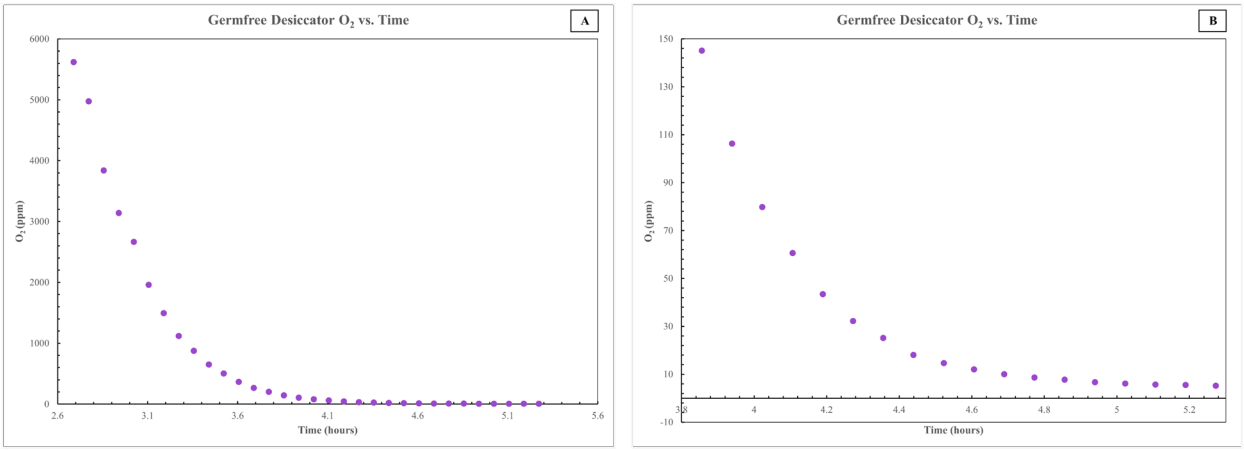

Fig 1: Chart A and B display O_2 ppm vs. time of a Germfree desiccator.

References

[1] Lauretta D. S. (2017) Space Sciences Reviews, 212, p. 925-984. [2] Watanabe S. (2017) Space Sciences Reviews, 208, p. 3-16. [3] Snead, C.J. (2024). LPSC LV, Abstract #2555. [4] FTM-PSt3/PSt6/PSt9 Metal Flow-Through Cell with Oxygen Sensor Instruction Manual, PreSens., Regenburg, Germany, p. 1-21.

Fine Particles and their origin in the Hayabusa2 clean chamber of the Extraterrestrial Sample Curation Center at JAXA

Yuma Enokido[1], Rei Kanemaru[1], Masahiro Nishimura[1], Ryota Fukai[1], Haruna Sugahara[1], Toru Yada[1], Arisa Nakano[1], Kasumi Yogata[1], Kentaro Hatakeda[2], Yuya Hitomi[2]
[1]*ISAS/JAXA*, [2]*Marine Works Japan Ltd.*

Introduction: The samples returned from C-type asteroid 162173 Ryugu are stored and handled in a pure nitrogen gas environment in the clean chamber (CC) in the Extraterrestrial Sample Curation Center (ESCuC) in Sagamihara to prevent alteration and contamination by Earth's atmosphere and surrounding materials [1]. The cleanliness of the samples in the CC has been controlled by restricting the use of materials of tools used in the CC, developing cleaning methods for them, and monitoring the environment. For example, humidity, oxygen, carbon dioxide, and methane levels are constantly monitored by Atmospheric pressure ionization-mass spectrometry (API-MS), which is directly connected to the CCs. Sampling the surface contaminants by placing quartz glass petri dishes in CC and following organic and inorganic mass spectrometry are also conducted several times a year (e.g. [2]). On the other hand, environmental monitoring focusing on the fine particles themselves, which are several tens to several hundred micrometers in size, has not been conducted systematically. In this study, we investigate fine particles in the CC where the samples returned from asteroid Ryugu are stored.

Methods: We collected particles attached to several Facility to Facility Transfer Containers (FFTCs) from CC4-1, which is utilized to store Ryugu samples. Samples to be allocated for other research institutes are packed in FFTCs and they are stored inside the CC until the timing of allocation. In this process, FFTCs are touched by gloves and other tools equipped with the CCs. The FFTCs used in this study are the ones stored in the CC for about half a year. We put the carbon tape to the outer wall surface of the FFTC at the clean room immediately after it was taken out from the CC, and the sticking particles were sampled. This method allows us to indirectly identify the particle present in the CC without contaminating the CC. The collected particles were observed by FE-SEM (SU6600: Hitachi High-Tech) equipped with an EDS detector. Some of them were mineralogically identified by Raman spectrophotometers (NRS-5100: JASCO). In addition, Ryugu samples (A0308 and C0054) were also observed to investigate the contamination on Ryugu particles. These samples were selected for publicity activities, and before loaning them to various institutions for display, basic data have been obtained by non-destructive analysis to explain the samples.

Results and Discussions: Most of the recovered particles from the surface of the FFTCs were several tens of micrometers in size, which were identified by analysis as aluminum alloy, SUS304, and silicates. Aluminum alloy and SUS304 are the main components of the CC and the handling tools used within CC. These results suggest that dust particles generated by friction between CC components (and tools) are deposited on the surface of the CC and stick to the gloves due to static electricity. Most of the silicates in recovered particles were identified as talc, chlorite, and wollastonite, and those materials are known as additives to Viton rubber in the manufacturing process. Fine particles originating from Viton gloves are also possibly generated by friction between gloves and between a glove and metallic tools.

SEM observations of Ryugu samples revealed that tiny fragments (tens of micrometers) of sapphire glass and SUS304 are attached to the sample surface. Sapphire glasses were observed on both samples (A0308 and C0054), and SUS304 fragments were observed only on C0054. Sapphire glasses were not observed as particles in the CC in this study. However, it is a material of the sample container and potentially exists as fine particles in the CC. C0054 was in contact with the CC floor during the initial description (classified as Class 2). Therefore, it is possible that the SUS304 particles, which were present on the CC floor, sticking to Ryugu samples.

Our result shows that even Class 2 Ryugu samples did not show a record of significant contamination. In addition, there is no previous study reporting these kinds of fine particles on the Ryugu samples except for this study. This is because the following measures were taken to reduce the possibility of contamination during sample handling: (1) Ryugu particles are kept in a covered container except during handling and analysis, (2) only the sample container (sapphire glass) and sample handling tools (vacuum tweezers, spatulas) are used to touch the Ryugu particles, and (3) The glove does not pass over the top surface of the sample during handling. We will establish a protocol for monitoring these particles on the CC surface and investigate better ways to reduce the frequency of particle generation. As the fine particles observed in this study are potential contaminants to the sample, it is important especially for samples classified as Class2 which are experienced to touch the surface of the CC and/or tools in the CC to investigate the influence on the sample analysis.

References

[1] Yada et al. Earth, Planets and Space (2023). [2] Hitomi et al. JAXA Special Publication (2023).

Terrestrial Alteration and Contamination on Previously Allocated Ryugu Samples

Rei Kanemaru[1], Kentaro Hatakeda[1,2], Yuma Enokido[1], Tomoko Ojima[1], Toru Yada[1], Kanako Sakamoto[1], Masahiro Nishimura[1], Ryota Fukai[1], Haruna Sugahara[1], Kasumi Yogata[1], Kana Nagashima[1], Rui Tahara[1], Arisa Nakano[1], Takuya Ishizaki[1], Seiya Kawasaki[1], Kazuya Kumagai[1,2], Hiromichi Soejima[1,2], Yuya Hitomi[1,2], Ayako Nakata[1], Yuriko Shimauchi[1], Ken Tamanoi[1], Akiko Miyazaki[3], Masanao Abe[1], Tatsuaki Okada[1], and Tomohiro Usui[1].

[1]*Astromaterials Science Research Group (ASRG), Institute of Space and Astronautical Science (ISAS), Japan Aerospace Exploration Agency (JAXA)*
[2]*Marine Works Japan Ltd*
[3] *Tokyo University*

Introduction

The samples returned from C-type asteroid 162173 Ryugu are handled in a pure nitrogen environment within the clean chamber (CC) at the Extraterrestrial Sample Curation Center in Sagamihara (ESCuC) to prevent alteration and contamination by Earth's atmosphere and materials [1]. The Ryugu particles are then allocated for initial analysis [e.g., 2, 3], Phase II curation [e.g., 4, 5], and Announcement of Opportunity (AO) research. During these studies, Ryugu samples are processed into various forms for analyses, such as polished sections (PTS), FIB sections, tiny particles attached to needles etc. These samples processing often involves handling with exposure to the atmosphere. Therefore, these Ryugu samples may have experienced alterations from their pristine state as that were stored in the CC. In this study, we investigated the previously allocated samples returned from research analysis to assess their terrestrial alteration and contamination. The previously allocated samples have been subject to reallocation to the AO research. Therefore, this study aimed to provide information that supports AO applicants in planning and executing their research projects, as well as to investigate methods for improving sample storage and preservation.

Samples and Methods

Previously allocated samples of eight particles (A0002-01, C0009-00, A0218-05, A0218-21, C0229-23, C0087-05, C0087-02, C0087-04) and two polished sections (C0014-02_PS, and C0087-06_PS) were selected for this investigation. After returned to the ESCuC, these samples are stored in a dedicated nitrogen-purged glove box (GB6). Exceptionally, the samples used in terrestrial weathering experiments [5] were stored in ambient condition in a clean room. In this study, the samples were classified into three types based on the handling history to assess the effects of atmospheric exposure: (1) non-atmospheric exposure, (2) short-term (less than a month), and (3) long-term (more than two years) atmospheric exposure. To investigate the effects of alteration in samples with different atmospheric exposure durations, we performed Fourier Transform Infrared Spectroscopic analyses using the IRT-5000 + FT/IR6100 (JASCO). Additionally, sample observations were conducted using a field-emission scanning electron microscope (FE-SEM, SU6600: Hitachi-High Tech.) equipped with energy-dispersive X-ray spectroscopy (EDS, Oxford AZtec Energy) to verify contamination caused by microparticles. All analyses were performed in a clean room. For the samples returned under non-atmospheric exposure conditions, all processes were completed without atmospheric exposure by using an airtight container during sample transfer. These results were compared with data obtained from pristine Ryugu particles (i.e., C0054 and A0308: outreach samples).

Results and discussion

Terrestrial Alteration of Previously allocated Ryugu particles

The μ-FTIR analysis was conducted on the several particle samples (Fig.1). This analysis revealed that all the previously allocated samples exhibit an asymmetric sharp absorption band centered at 2.7 μm with broad absorption of 2.8-3.2 μm, while pristine Ryugu particles (C0054 and A0308) have only a sharp absorption centered at 2.71 μm. Non-atmospheric exposure and short-term exposure samples show the same state in depth of the absorption band at 2.8 to 3.2 μm, and deeper absorption in long-term exposure samples. Generally, absorption around 3.0 μm is associated with water (i.e., H_2O) absorption from ambient air. This could be attributed to the increased adsorption of water on the sample due to prolonged atmospheric exposure. This study also presented that even the non-atmospheric exposure samples were affected by terrestrial atmosphere during sample handling, analysis, and/or transportation. In the observation by SEM-EDS, we confirmed the

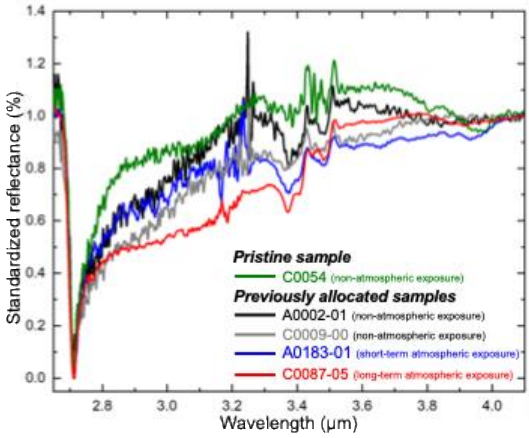

Fig. 1. Standardized FTIR spectra of selected Ryugu particles. All previously allocated Ryugu particles has broader absorption band than pristine particle.

precipitation of gypsum in long-term exposure samples (both particle and PTS) which were already reported in the same sample by [5] and this is considered as the result of terrestrial alteration by Earth's atmosphere (Fig. 2). No growth of gypsum was observed in these samples since the last observation in January 2023 [5]. On the other hand, gypsum was not observed in non-exposure and short-term exposure samples.

Contaminant microparticles on Previously allocated Ryugu samples

We often find C-rich microparticles in all particles and polished sections in the investigated previously allocated samples by SEM-EDS observation. Many of these microparticles are rich in carbon and nitrogen, which are considered to be organic matter. Organic molecules have been found in Ryugu particles, but the observed microparticles are attached on the sample surface and we have not observed them in that shape in pristine particles. Therefore, we interpret these C-rich microparticles were contaminated during the sample processing and/or analysis. Another type of C-rich microparticles were found in a particle after extraction of FIB sections. They are spherical shaped and rich in carbon and magnesium, and are likely the mixture of deposition liquid and sample material melted by irradiation of ion beam in the FIB sectioning process.

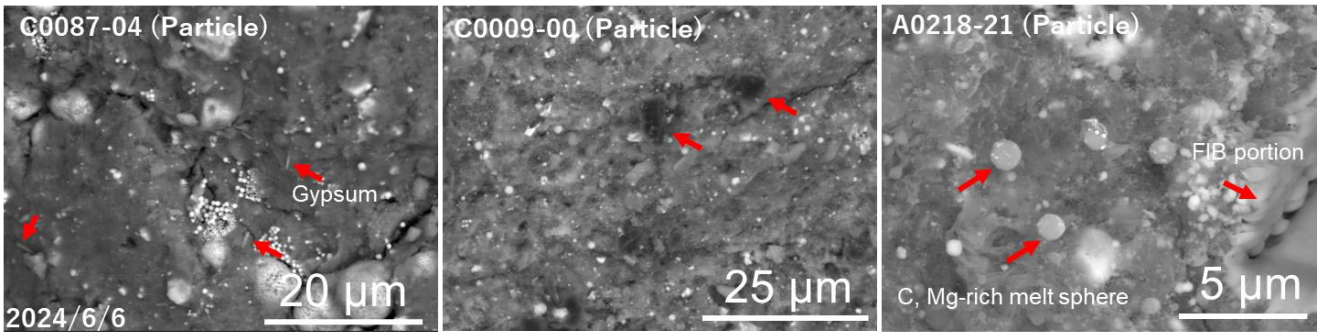

Fig. 2. BSE images of selected samples studied here. C0087 that used terrestrial weathering experiments contains lathy gypsum. The C-rich particles are present on the surface of the previously allocated samples (both particles and PTS). Additionally, C, Mg-rich particles, likely formed during the FIB process, are frequently observed near the FIB portion.

Summary

This study briefly evaluated the effects of terrestrial atmosphere on Ryugu particles using the previously allocated samples of different exposure time. We also found C-rich microparticles on the surface of the investigated samples as possible contaminants. As the previously allocated samples are available for reallocation to AO research, the results of this study are expected to be useful for researchers when selecting the adequate samples according to their research purpose. Especially, caution is required for considering spectroscopy and organic geochemistry for these samples. Further study is needed to understand the detailed effect of terrestrial atmosphere on samples returned in sample return missions, and more information is needed to assess the potential of contamination during the sample processing and analysis. These would contribute to improve the knowledge and techniques of astromaterials sample curation in ESCuC.

Acknowledgment

We are grateful to the Phase II Kouchi team for providing detailed information about the investigated samples and to their helpful comments on the results.

References: [1] Yada. T. et al. Preliminary analysis of the Hayabusa2 samples returned from C-type asteroid Ryugu. *Nat. Astron.* **6**, 214-220 (2021) [2] Nakato. A. et al. Variations of the surface characteristics of Ryugu returned samples. *EPS.* **75**, 45 (2022) [3] Nakamura. T. et al. Formation and evolution of carbonaceous asteroid Ryugu: Direct evidence from returned samples. *Science.* **379**, 6634 (2022) [4] Ito. M. et al. A pristine record of outer Solar System materials from asteroid Ryugu's returned sample. *Nature.* **6**, 1163-1171 (2022) [5] Imae. N. et al., Mineralogical approach on laboratory weathering of uncontaminated Ryugu particles: Comparison with Orgueil and perspective for storage and analysis. *MAPS.* **59**, 7, 1705-1722 (2024).

The terrestrial weathering processes of Ryugu grains

M. Miyahara[1], T. Noguchi[2], T. Matsumoto[2], N. Tomioka[3], A. Miyake[2], Y. Igami[2], Y. Seto[4],
[1]*Hiroshima Univ., Japan*; [2]*Kyoto Univ., Japan;* [3]*JAMSTEC, Japan;* [4]*Osaka Metropolitan Univ., Japan*

Introduction: The Hayabusa2 analysis teams show that the Ryugu grains consist mainly of a matrix: saponite and serpentine along with small amounts of magnetite, iron sulfides, carbonates, and phosphates (Nakamura et al., 2023; Noguchi et al., 2024). The mineralogical and geochemical characteristics of the Ryugu grains are most similar to the CI chondrites (Ito et al., 2022; Nakamura et al., 2023; Yokoyama et al., 2023). CI chondrites are the most difficult to recover on earth as meteorites due to their friability. After falling to earth, the fragments are affected by terrestial weathering (reactions between a rock and air/water) and gradually lose the original characteristics of CI chondrites. An Antarctic meteorite may be less affected by terrestrial weathering because the meteorites were stored in an ice field after the fall. However, based on terrestrial ages by cosmogenic radionuclides, the average residence time of Antarctic meteorites is about 10^5 years (Nishiizumi et al., 1989). A reaction between terrestrial water/ice and meteorites would continue even in an Antarctic ice field (Bland et al., 2006), so it is difficult to clarify intrinsic aqueous alteration that occurred on a parent body using only meteorites.

How the terrestrial weathering of CI chondrites proceeds should be clarified to understand the intrinsic aqueous alteration that occurred in C-type asteroids. However, we cannot clarify the terrestrial weathering process only by artificial alteration experiments on CI chondrites, because as mentioned above, most meteorites have spent a long time in terrestrial conditions after the fall. We propose to clarify the early stage terrestrial weathering process of CI chondrites by using the Ryugu grains. In this research project, Ryugu grains will be exposed to the atmosphere for a long time, and changes in the surface of the grains will be repeatedly observed by FEG-SEM. In the final stage, cross-sectional observations near their surfaces will be made with a TEM to clarify how the initial stages of terrestrial weathering of CI chondrites proceed.

Sample histories and experimental methods: The sample plate C0105-042_000_00 (hereinafter referred to as C0105-042), which was once analyzed by the Hayabusa2 Initial Analysis "Sand" team and reassigned by the approval of the 2nd AO, was used for this research. Ryugu small grains on C0105-042 were observed by secondary electron (SE) imaging (at a low accelerating voltage of 3.0–5.0 kV) to investigate the surface morphology using a FEG-SEM. The first and second FEG-SEM observations were performed without any coating. After the second observation (26 days after the arrival of the sample to the "Sand" team), Ryugu small grains on C0105-042 were coated with carbon after osmium. After the third observation (149 days after the arrival of the sample to "Sand" team), the C0105-042 plate was returned once to JAXA following the completion of the initial analysis group's activities. C0105-042 had been stored in a vacuum desiccator except for the FEG-SEM observations.

The fourth observation (497 days after the first arrival of the sample to the "Sand" team) was performed immediately after the realocation of C0105-042. After the fourth observation, C0105-042 was exposed to the atmosphere in a special desiccator installed in a clean room. The temperature and humidity in the desiccator were maintained at approximately 20–23°C and 30–40%. After the beginning of the atmospheric exposure, the fifth and sixth FEG-SEM observations were performed 104 and 245 days later, respectively. After the sixth observation, C0105-042 was placed in a vacuum desiccator to complete the atmospheric exposure experiment. After being coated with osmium and carbon to prevent Ga-ion damage to the grain surface, several portions of the Ryugu small grains were excavated by an FIB device and processed into TEM ultrathin films to study their terrestrial weathering processes.

Results and discussion: FEG-SEM observations of C0105-042 immediately after the reallocation by JAXA show that the morphology of the grain surface had changed significantly, even though the sample had been stored in a nitrogen-filled desiccator. In some of the grains where cracks had observed at the initial analysis period, the width of the cracks was even larger, and some of the grains were broken into smaller pieces. Numerous fine-grained precipitates about 100 nm or less in size were formed on the surface of Mg-Fe phyllosilicates, magnetite, dolomite, and pyrrhotite. Mycelial-like precipitates less than about 500 nm in length were formed in the spaces between the magnetite particles. Amoeboid precipitates covered the surface of iron sulfide particles. As the exposure time of the Ryugu grains to the atmosphere increased, some of the Ryugu small grains that had developed wide cracks fell out completely. The Ryugu small grains have been completely covered with fine-grained precipitates layers and the size has become coarser (>200–300 nm). All pyrrhotite particles were completely covered with amoeboid precipitates. Therefore, it is difficult to observe their original outlines.

TEM images show that fine-grained precipitate layers covering the entire Ryugu grains consist of amorphous or poorly crystallized materials. Based on the EDS spectra, the precipitates are mainly composed of carbon and oxygen with a small amount of silicon and magnesium. The average thickness of the precipitate layers is approximately 100 nm. Evidence of alteration was observed in the pyrrhotite particles near the Ryugu grain surface, although not exposed on the surface: i.e., the edges of the pyrrhotite particles are depleted in sulfur. Sulfur released from pyrrhotite has not been confirmed around the particles. The volume fraction of the altered portion increases as the pyrrhotite particle size decreases. For a pyrrhotite particle with a diameter of about 30 nm, the volume fraction of the altered portion is 70% or more. Around the altered pyrrhotite particles, froth-like textures are observed in carbonaceous materials. The amoeboid precipitates on a pyrrhotite single crystal are amorphous or poorly crystallized materials depleted in iron along with sulfur compared to the original pyrrhotite. EDS analyses clarified that the amoeboid precipitates are oxidized or hydrated. The average thickness of the amoeboid precipitate layer is about 450 nm.

Under oxic acidic conditions, pyrrhotite can dissolve rapidly and generate Fe^{2+} and H_2S, although the dissolution rate decreases under neutral and alkaline conditions (Belzile et al., 2004). The absence of sulfur (S_0) and sulfate (SO_4^{2-}) around the altered pyrrhotite particles may support the generation of H_2S by the dissolution reaction under oxic conditions. Froth-like texture,

which are present in the carbonaceous materials around the altered pyrrhotite particles, may indicate degassing of CO_2 due to the reaction between H_2S and the carbonaceous materials. The alteration rate was calculated using a pyrrhotite single crystal completely exposed to air, given the time of exposure to air and the thickness of the alteration layer. The estimated alteration rate is about 2 nm/day. This alteration rate is upper limit because a small amount of amoeboid precipitate was present on the surface prior to the exposure experiment.

The estimated formation rate of fine-grained precipitate layers covering the entire Ryugu grains is about 0.5 nm/day. The origin of the fine-grained precipitate layers is not clear at this time. There are two possible scenarios to explain the origin. In scenario 1, the dissolved intrinsic carbonaceous material are reprecipitated on the grain surface. Carbonaceous materials around pyrrhotite particles are dissolved by H_2S. The dissolved carbonaceous materials may migrate and precipitate on the surface of the Ryugu grains. In scenario 2, extrinsic carbonaceous materials are precipitated on the surface of the Ryugu grains. Epoxy resin used to adhere the Ryugu grains to an Au plate or unknown materials including carbon, probably from a decicator, may cause contamination.

Current exposure experiments show that the terrestrial weathering of the Ryugu grains has proceeded from the surface to the interior, but their detailed chemical reactions are not clear. Imae et al. (2024) also conducted the terrestrial weathering experiments on Ryugu grains and reported that small-sized euhedral Ca-sulphate particles on the surface. Such alteration products has not been found in our exposure experiments. Further investigations, such as the speciation of sulfur and iron, are needed to clarify the terrestrial weathering processes of Ryugu grains.

References

Belzile et al. (2004) A review on pyrrhotite oxidation. *Journal of Geochemical Exploration* **84**, 65–76.

Bland et al. (2006) Weathering of chondritic meteorites. University of Arizona Press, Arizona. pp. 942.

Imae et al. (2024) Mineralogical approach on laboratory weathering of uncontaminated Ryugu particles: Comparison with Orgueil and perspective for storage and analysis. *Meteoritics & Planetary Science* **59**, 1705–1722.

Ito et al. (2022) A pristine record of outer solar system materials from asteroid Ryugu's returned sample. *Nature Astronomy* **6**, 1163–1171.

Nakamura et al (2023) Formation and evolution of carbonaceous asteroid Ryugu: Direct evidence from returned samples. *Science* **379**, eabn8671.

Nishiizumi et al. (1989) Update on terrestrial ages of Antarctic meteorites. *Earth and Planetary Science Letters* **93**, 299–313.

Noguchi et al. (2024) Mineralogy and petrology of fine-grained samples recovered from the asteroid (162173) Ryugu. *Meteoritics & Planetary Science* **59**, 1877–1906.

Yokoyama et al. (2023) Samples returned from the asteroid Ryugu are similar to Ivuna-type carbonaceous meteorites. *Science* **379**, eabn7850.

Analysis of Ryugu Fluid Inclusions: An Update

Andrei Dolocan[1], Robert Bodnar[2], Michael Zolensky [3], JangMi Han[4], Romy Hanna[1], Iona Gearba[1], Queenie Chan[5], Trevor Ireland[6], Loan Le[4], Megumi Matsumoto[7], Akira Tsuchiyama[8].
[1]Univ. of Texas, Austin TX 78712, USA (adolocan@austin.utex.edu); [2]Virginia Tech, Blacksburg VA 24060, USA; [3]ARES, NASA Johnson Space Center, Houston, TX 77058, USA; [4]Jacobs Tech., Houston, TX 77058, USA; [5]Royal Holloway University, Egham TW20 0EX, UK; [6]University of Queensland, St Lucia 4072, Queensland, Australia; [7]Tohoku University, Aoba-ku, Sendai, Miyagi, Japan; [8]Ritsumeikan Univ., Kusatsu, Shiga, 525-8577, Japan.

Introduction: The most direct and convincing evidence for the presence of water and organic molecules on protoplanetary bodies is provided by fluid inclusions trapped in secondary minerals [1]. Our previous work has demonstrated that early solar system fluids have survived as fluid inclusions in a Ryugu pyrrhotite crystal [2]. We hypothesize that the bulk molecular and isotopic composition of individual Ryugu fluid inclusions can be measured to provide ground truth for exploring and thermochemical modeling of the compositional and isotopic evolution of fluids in protoplanetary bodies including asteroids, comets and icy moons.

This presentation is an update on our efforts to make measurements of elemental, molecular and, in particular, isotopic compositions of individual aqueous fluid inclusions in Ryugu samples. The measurements we plan will permit us to (1) understand elemental composition of the aqueous fluids present on Ryugu's progenitor body, (2) track changes in the chemical and stable isotopic composition of altering fluids in small bodies over time, (3) verify the presence of organics in Ryugu fluids, (4) verify the reported significant CO_2 in Ryugu fluids, (5) measure O and H isotopes in preserved Ryugu fluids, (6) provide constraints on temperature range calculations for the mineralizing reactions being performed by other groups using mineral pairs, (7) measure sulfur/chloride and chloride/phosphorus ratios of Ryugu fluids. We note here that recent results from Enceladus reveal the importance of phosphorus in small body aqueous brines [3], indicating that our proposed research will benefit studies of all current ocean worlds.

Facilities: For the following XRCT and TOF-SIMS analysis, samples were prepared using the FEI Quanta 3D 600 Dual-beam Focused Ion Beam in the ARES -NASA-JSC Electron Beam Instrument Facility. For the X-ray Computed Tomography (XRCT) scans we used the Zeiss 620 XRM instrument at the University of Texas High-Resolution X-ray Computed Tomography Facility. For the Time of Flight-Secondary Ion Mass Spectrometry (TOF-SIMS) measurements we used the University of Texas Materials Institute's TOF-SIMS 6 instrument (ION-TOF GmbH) equipped with a pulsed Bi^+ analysis ion beam (30 keV ion energy) and a O_2^+ sputtering ion beam (1 kV ion energy). This TOF-SIMS instrument is capable of cooling the samples to -180ºC, and without this capability our measurements would be impossible.

Ryugu Fluid Inclusion Measurements: Our recent successful, coordinated, XRCT and TOF-SIMS analyses of individual fluid inclusions in a Ryugu pyrrhotite crystal demonstrated that they consist of water, CO_2, sulfur species, and organic material, with H^-, C^-, O^-, S^- and OH^- as the main fragments detected at these locations [2]. In addition, various amounts of F^-, Cl^- and Ni^- were found, together with Na^+, Mg^+, Al^+, Cr^+, K^+ and Ca^+. Larger organic fragments such as C_2^-, C_2H^-, C_3^-, CO^- and CN^- were also detected, indicating the presence in these inclusions of more complex organic molecules containing H, C, N and O. We can expect to see these and additional molecular fragments in other Ryugu fluid inclusions. TOF-SIMS breaks apart molecules - it does not make new ones. Therefore, all these identified species are fragments of once larger molecules which we can identify to some degree.

We made XRCT scans of Ryugu grains (A0175 and C0043) (Fig. 1). From these preliminary measurements we know that A0175 contains numerous pyrrhotite, carbonate, and, probably, apatite crystals with fluid inclusion candidates measuring at least 3-5 μm in diameter, which will permit our planned TOF-SIMS measurements.

Stable isotope Measurements: In the past year we have begun isotopic measurements of standards. This task has required use of the few well-characterized standard materials that are isotopically homogeneous at the sub-micron scale. There are few of these available at the current time. In preparation for addressing the Ryugu samples, we first measured the hydrogen and oxygen isotopic composition of synthetic fluid inclusions in halite using the M6 TOF-SIMS instrument in high mass resolution mode. The halite standards were prepared by Bob Bodnar and have trapped fluids with D/H of 0.0005 but unknown $^{18}O/^{16}O$. With continued calibration effort we will determine the instrumental mass fractionation for this instrument, but already we have learned that the hydrogen isotopes are best measured by setting the analysis gun in "Fast Imaging" High Spatial Resolution Mode, while setting the analysis gun in "Spectrometry" mode and keeping the analyzer in "All Purpose" increasing the mass resolution in "All Purpose" mode

(All Purpose Resolution, an optimal setting between high mass and high spatial resolution) is best for oxygen. These results will now permit us to revisit the fluid inclusions found in halite in the Monahans (1999) and Zag meteorites, permitting new D/H measurements to be made (this was preciously done by S. Itoh, Y. Yurimoto and coworkers [4]).

For O isotope measurements in Ryugu samples will use the UWQ-1 quartz standard developed at the University of Wisconsin [5] and provided by John Valley and Noriko Kita. Our initial session with this standard resulted in a measurement standard deviation of 5‰ for ^{18}O and ^{16}O. Unfortunately, we probably cannot usefully measure ^{17}O in our samples because of mass interference with ^{16}OH. Measurements of oxygen at a high mass resolution mode might result in usable results for ^{17}O, however we cannot operate at that mode for individual fluid inclusions, which generally require measurements to be made in a high spatial resolution mode. Fortunately, the two oxygen isotopes we can measure are sufficient to permit comparisons to be made with ongoing work on Ryugu solid mineral pairs (see [6-8]), such as dolomite/magnetite, by other groups with whom we are in regular contact (e.g. H. Yurimoto's and R. Greenwood's groups). This is important as the results for Ryugu samples to date are either in conflict or indicate a rather wide range of mineralizing solution temperatures, namely ~25°C by Greenwoods group [9] and ~100°C by Yurimoto's group [8].

For hydrogen isotope measurements we are currently using MORB SR02 glass provided by Laurette Piani (Centre de Recherches Pétrographiques et Géochimiques (CRPG), Nancy), which was developed by Etienne Deloule. This sample has the following composition: H_2O = 2600 ± 110 wt. ppm and deltaD = -81.8 ± 5.3 ‰. Using the M6 TOF-SIMS we have succeeded in measurements of D/H in this glass with a measurement standard deviation of 33‰. This result is adequate for our purposes.

Next Steps: Thus, the isotopic measurements we propose will take effort, but we can successfully make them. In the next 6 months we will begin to measure hydrogen and oxygen isotope concentrations in individual Ryugu fluid inclusions, beginning with pyrrhotite crystals first scanned by XRCT by Romy Hanna (Univ. Texas). These sulfides contain no structural oxygen and are thus well suited for oxygen isotope measurements, since we will not have to analytically separate counts from the oxygen secondary ion signal in the host minerals from the oxygen signal in the trapped fluids during data reduction.

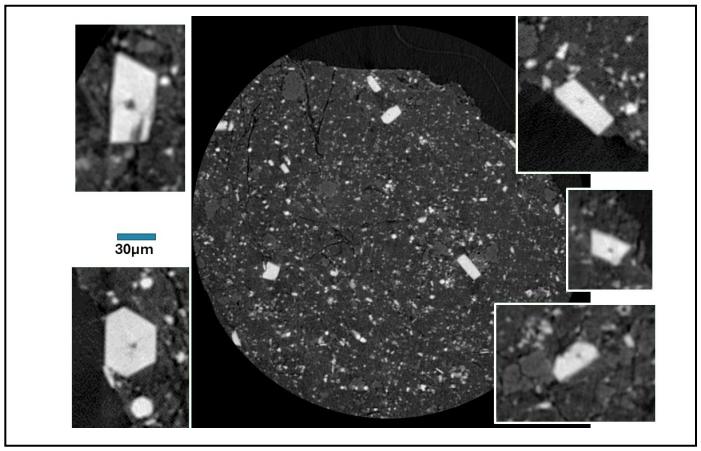

Figure 1. (Center) Portion of frame of the XRCT scan of Ryugu particle AO175, exhibiting numerous large pyrrhotite crystals (white). This sub-scan measures approximately 0.5 mm across. Set around the central image are higher magnification scans of pyrrhotite crystals identified in the particle, all at the same magnification. Probable fluid inclusions are visible as dark spots in the centers of each pyrrhotite crystal.

Acknowledgements: We thank JAXA for Ryugu samples, and the NASA Hayabusa2 Participating Scientist Program. Funding was provided by a NASA LARS Program grant to MZ. We thank Noriko Kita, John Valley, Laurette Piani, Rhonda Stroud and Larry Nittler for valuable discussions and standards.

References: [1] Bodnar et al. (2019) *50th LPSC Abstracts*; [2] Nakamura et al. (2022) *Science* **377**, 10.1126/science.abn8671; [3] Postberg et al. (2023) *Nature* **618**, 489–493; [4] Yurimoto et al. (2014) *Geochem. J.* **48**, 1-12; [5] Kelley et al. (2007) *GCA* **71**, 3812-3832; [6] Zheng (1991) *GCA* **55**, 2299–2307; [7] Zheng (2011) *Geochem. J.* **45**, 341-354; [8] Yokoyama et al. (2023) *Science* **379**, eabn7850; [9] Greenwood et al. (2023) *Nature Astronomy* **7**, 29-38.

The Mineralogy of Asteroid Bennu from X-ray Diffraction Analysis

A. J. King[1], V. Tu[2], P. F. Schofield[1], J. Najorka[1], S. S. Russell[1], H. C. Bates[1], T. J. Zega[3], T. J. McCoy[4], L. P. Keller[5], P. Haenecour[3], M. S. Thompson[6], K. Thomas-Keprta[7], L. Le[2], D. P. Glavin[8], J. P. Dworkin[8], H. C. Connolly Jr.[3,9,10], and D. S. Lauretta[3]

[1]*Natural History Museum, London, UK (a.king@nhm.ac.uk); [2]Jacobs, NASA JSC, Houston, TX, USA; [3]Lunar & Planetary Laboratory, University of Arizona, Tucson, AZ, USA; [4]National Museum of Natural History, Smithsonian Institution, Washington, D.C., USA; [5]NASA JSC, Houston, TX, USA; [6]Purdue University, West Lafayette, IN, USA; [7]Barrios Technology/Jacobs, NASA JSC, Houston, TX, USA; [8]NASA GSFC, Greenbelt, MD, USA; [9]Rowan University, Glassboro, NJ, USA; [10]American Museum of Natural History, New York, NY, USA.*

Introduction: Carbonaceous asteroids likely played an important role in the delivery of water and organic matter to the early Earth [e.g. 1]. Fragments of these bodies naturally arrive on Earth as meteorites that can be studied in the laboratory. However, meteorites often lack geological context and are rapidly modified in the terrestrial environment [e.g. 2]. On September 24, 2023, NASA's OSIRIS-REx mission delivered to Earth a pristine sample collected from the surface of the carbonaceous asteroid Bennu. Remote observations indicated that Bennu consists of abundant phyllosilicates, carbonates, oxides, and carbon, similar to the composition of highly aqueously altered carbonaceous chondrites [3]. This prediction was initially confirmed during a "quick-look" analysis of fine dust coating the avionics deck of the sample canister and the outside of the sample collector [4]. Here, we characterise the mineralogy of returned samples using X-ray diffraction (XRD) and discuss its implications for understanding the geological history of Bennu.

Samples & Methods: Bennu sample OREX-500005-0 (~88 mg), which mainly consists of fine (<100 μm) particles recovered from the avionics deck, was mounted onto a zero-background substrate, and XRD patterns were acquired (ambient conditions, Co K_α radiation) using a Malvern Panalytical X'Pert Pro scanning XRD instrument at NASA Johnson Space Center (JSC). OREX-800107-103 (~49 mg), a sub-sample of a larger (~6 g) aggregate of material from inside the sample collector, was powdered and homogenised at JSC. This sample was packed into an aluminium well and then analysed (ambient conditions, Cu $K_{\alpha1}$ radiation) using an INEL XRD with a curved 120° position-sensitive-detector at the Natural History Museum, London.

Results: XRD patterns for OREX-500005-0 and OREX-800107-103 show that both samples contain abundant phyllosilicates, with relatively broad reflections (~12.4, ~7.3, ~4.6, ~3.6, and ~1.5 Å) attributed to Mg-serpentine and Mg-smectite. Other phases identified include magnetite, Fe-sulfides (pyrrhotite + pentlandite), and carbonates (dolomite + calcite), plus a small, sharp diffraction peak that is likely from olivine. Diffraction peaks from Mg,Na-phosphate, which appears as bright phases in the Bennu samples [4], were not detected, possibly because it is poorly crystalline/amorphous [5, 6]. We also found no evidence for sulfate or Fe-(oxy)hydroxide phases. Quantitative phase analysis gives a bulk mineralogy of ~70 – 80 vol.% phyllosilicate, ~10 – 15 vol.% Fe,Ni sulfide, ~5 – 10 vol.% magnetite, <5 vol.% carbonate, and trace amounts of olivine. Based on the bulk mineralogy, we estimate that the Bennu samples have a grain density of ~2.8 – 3.0 g cm^{-3} and a porosity of ~40 % (assuming a bulk density of ~1.7 g cm^{-3} [4]).

Discussion: The similarity of the XRD patterns for OREX-500005-0 and OREX-800107-103 suggests that the fine dust outside of the sample collector is mineralogically representative of the bulk Bennu sample within it. Furthermore, the scarcity of sulfates [6] and absence of Fe-(oxy)hydroxides, which in carbonaceous chondrites are usually attributed to terrestrial weathering, confirms the pristine nature of the returned materials. Overall, the mineralogy of OREX-500005-0 and OREX-800107-103 indicates that Bennu's parent body experienced hydrothermal alteration. This body must have accreted water ice, with melting resulting in extensive water-rock reactions that transformed most of the original minerals into a secondary assemblage of phyllosilicates, oxides, Fe,Ni sulfides, and carbonates. The phyllosilicate fraction (total phyllosilicate abundance / [total anhydrous silicate + total phyllosilicate abundance]) corresponds to a petrologic sub-type of 1.1 [7], comparable to most aqueously altered meteorites [8] and samples returned from asteroid Ryugu by the Hayabusa2 mission [9]. However, the estimated low density and high porosity of the Bennu samples [4, 10] suggests that they would not easily survive passage through Earth's atmosphere, as was previously suggested for the weak boulders identified on Bennu's surface [11].

Supported by NASA Award NNH09ZDA007O and Contract NNM10AA11C issued through the New Frontiers Program.

References

[1] Alexander C. M. O'D. et al. (2012) Science 337:721. [2] Jenkins L. E. et al. (2024) M&PS 59:988. [3] Hamilton V. E. et al. (2019) Nat. Astron. 3:332. [4] Lauretta D. S., Connolly Jr. H. C. et al. (2024) M&PS 59:2453. [5] Barnes J. J. et al. (2024) 55th LPSC Abstract #1532. [6] McCoy T. J., Russell S. S. et al. in review. [7] Howard K. T. et al. (2015) GCA 149:206. [8] Russell S. S. et al. (2022) M&PS 57:277. [9] Nakamura T. et al. (2022) Science 379:eabn8671. [10] Ryan A. J. et al. (2024) 55th LPSC Abstract #1594. [11] Rozitis B. et al. (2020) Sci. Adv. 6:eabc3699.

Constraining the Temperature-pH Space of Aqueous Fluids on Bennu's Parent Asteroid Based on the Major Mineralogy of the OSIRIS-REx Returned Samples

V.R. Manga[1,2], M.K. Kontogiannis[1], T.J. Zega[1,2], L.P. Keller[3], H.C. Connolly[1,3,4], T.J. McCoy[5], S.S. Russell[6], D.S. Lauretta[1]

[1]Lunar and Planetary Laboratory (manga@arizona.edu), [2]Department of Materials Science and Engineering, University of Arizona, Tucson, AZ, USA, [3]Astromaterials Research and Exploration Science Division, Johnson Space Center, NASA, Houston, TX, USA, [4]Department of Geology, Rowan University, Glassboro, NJ, USA, [5]Department of Earth and Planetary Sciences, American Museum Natural History, New York, NY, USA, [6]Department of Mineral Sciences, National Museum of Natural History, Washington, DC, USA, [7]Planetary Materials Group, Natural History Museum, London, UK.

Introduction: The mineralogy of Bennu samples returned by OSIRIS-REx reveals extensive aqueous processing of precursor rocks, indicating substantial fluid on the parent asteroid [1,2]. The major phases are hydrated phyllosilicates (e.g., serpentine and saponite), sulfides (e.g. pyrrhotite), magnetite, carbonates and phosphates. These phases can form through direct precipitation within such a fluid. In addition, microstructural features such as carbonate veins and phyllosilicates of different morphologies point to spatial and temporal heterogeneities in the fluid evolution [3,4]. Our computational work aims to model the fluid phase that mediated the mineralogical evolution. We conduct thermodynamic modeling of the multi-component aqueous system, FeS-NiS-MgO-SiO_2-CaO-H_2O, to constrain the temperature-pH space of precipitation of the major minerals. This work will help test the hypothesis that the hydrothermal reactions occurred between 25 to 375 °C [5].

Methods: The computational framework includes *ab initio* and classical approaches to predict thermochemistry of the condensed phases, i.e., the solid [6,7] and aqueous solutions. Atomistic simulations also investigate freezing-point depression and fluid speciation in the range of 0 to –100 °C. Thermodynamic modeling of the solution phases is conducted within the CALPHAD (CALculation of PHAse Diagrams) framework by combing the available thermochemical and phase diagram data from literature and from this work. As a first step, the existing thermodynamic databases are employed to predict the precipitation sequences and aqueous phase diagrams to help interpret the results from sample analysis.

Results and Discussion: The calculated Pourbaix diagram of the Si-Mg-Ca-Ni-Fe-S-C-H_2O system at 25°C and a water-to-rock ratio 2:1, showed a phase region with the major minerals (serpentine+pyrrhotite+$CaCO_3$+magnetite) to be stable in the pH range of 6 to 8.2. Increased water-to-rock ratio is found to shift the pH range of the phase field of the major minerals to higher basicity. The results are analyzed in comparison to conditions modeled for Ryugu and CI chondrites [8,9]. We will discuss the implications of these results for parent-body processing, including the precipitation sequence and the possibility of alteration at <0 °C.

Acknowledgements: The research is supported by NASA under Contract NNM10AA11C issued through the New Frontiers Program. The computational work is enabled by the supercomputing resources provided by the NASA High-End Computing (HEC) Program through the NASA Advanced Supercomputing (NAS) division at Ames Research Center. The authors are also grateful for the high-performance computing (HPC) facility at the University of Arizona.

References: [1] Lauretta D.S. et al. (2022) *Science* 377:285-291. [2] Lauretta D.S., Connolly H.C. et al. (2024) *Meteoritic and Planetary Science* 59:2453-2486. [3] Almeida N.V. et al. (2024) *LPSC LV*, Abstract #1521. [4] Zega et al. (2024) *Meteoritic Society* Abstract #6450 [5] Lauretta D.S. et al. (2023) arXiv [astro-ph.EP] 2308.11794. [6] Kresse G. and Joubert J. (1999) *Phys. Rev. B* 59:1758-1775. [7] Perdew J.P. et al. (1996) *Phys. Rev. Lett.* 77:3865-3868. [8] Nakamura T. et al. (2022) *Science* 379:eabn8671. [9] Zolensky M. et al. (1989) *Icarus* 78:411-425.

Shock metamorphic effects in the Ryugu carbonates

E. Dobrică[1], K. Nagashima[1], G. R. Huss[1], A. N. Krot[1] and A. J. Brearley[2]
[1]*Hawai'i Institute of Geophysics and Planetology, University of Hawai'i at Mānoa, HI, USA;* [2]*Department of Earth and Planetary Sciences, University of New Mexico, NM, USA.*

Introduction: Carbonates have traditionally been used to constrain the chemical evolution of fluids and the duration of aqueous alteration processes [1]. However, recent studies have shown that carbonates are also valuable recorders of shock metamorphic environments and help interpret shock metamorphic conditions on the chondrite parent asteroids [2-3]. Evidence of mild shock metamorphism, with an average peak pressure of ~2 GPa, has been reported in samples returned from the surface of the asteroid (162173) Ryugu by the JAXA Hayabusa2 spacecraft [4]. Only a small fraction of the material, around 0.2 vol%, experienced higher shock pressures exceeding 10 GPa during impact [5]. In this study, we focus on the effects of shock metamorphism on the carbonates identified in the Ryugu samples. Notably, three types of carbonates (calcite, dolomite, and magnesite) have been commonly observed in the main lithologies of Ryugu [6], with abundances reaching up to 4.4 vol% [5]. Calcite, though rare, has been identified in isolated clasts from chamber C, where it coexists with primary anhydrous silicate minerals such as Mg-rich olivine and pyroxene [7]. Isotopic measurements of oxygen and carbon indicate that most calcite precipitated first, followed by dolomite [7]. A key objective of our research is to determine whether carbonates formed from different fluid sources exhibit varying degrees of shock metamorphic alteration.

Samples and methods: We conducted an integrated study using scanning electron microscopy (SEM) and focused ion beam/transmission electron microscopy (FIB/TEM) to observe and analyze two Ryugu particles (A0104 and C0030), collected during the two touchdowns of the Hayabusa2 spacecraft in chambers A and C, respectively. We selected four regions containing the three different types of carbonates (calcite, dolomite, and Mn-rich magnesite) identified so far in the Ryugu samples for detailed analysis. The electron-transparent sections (three FIB sections from C0030 and one FIB section from A0104, designated A0104-026087) were prepared using the Helios 660 FIB-SEM instrument at the University of Hawai'i at Mānoa and examined by TEM using the JEOL NEOARM 200CF at the University of New Mexico.

Results and discussion: Our study reveals that two calcites from sample C0030 show no defects or evidence of shock metamorphism or space weathering (Fig. 1a, c-e). In contrast, the calcite from A0104 (Fig. 1b) exhibits radial dislocations throughout the crystal, many of which have split into partial dislocations [8], likely as a mechanism to reduce stress. This calcite is associated with Mg-rich olivine (Fo_{100}), similar to that described in less altered clasts by [7]. In general, all calcites display post-precipitation modifications, indicating interactions with fluids of varying compositions, both extraterrestrial and terrestrial. These alterations appear as heterogeneous, euhedral rims—either Mn-rich (Fig. 1b) or with calcium sulfate overgrowths up to 500 nm thick (Fig. 1a). The calcium sulfate likely formed within a relatively short timeframe, possibly less than a year of exposure to terrestrial conditions [9], despite the sample being stored in desiccators. Additionally, sodium-enriched regions (5.6 wt.% Na_2O) at the calcite grain boundary suggest later diffusion and further alteration after precipitation. This calcite is also associated with Mg- and Na-rich amorphous phosphate and Mn-rich magnesite [$Mg_{1.0}Mn_{0.8}Ca_{0.3}Fe_{0.3}(CO_3)_2$]. The Mn-rich magnesite exhibits modulations and strain contrast, possibly formed during crystal growth or shock metamorphism [3], and shows compositional heterogeneity with an FeO-rich rim and CaO-rich/CaO-poor zones (Fig. 1d-e).

We also prepared a FIB section of a large dolomite associated with other secondary phases such as apatite (Cl- and F-poor hydroxyapatite) and framboidal magnetite (Fig. 1f-g). In this section, two generations of dolomite were identified. The larger dolomite contains numerous pores and embayments, sometimes filled with phyllosilicates. Multiple signs of shock have been identified in this mineral, such as numerous dislocations, stacking faults, and parallel dislocations in multiple directions, similar to those observed in carbonates affected by shock metamorphism in CMs and Antarctic micrometeorites [2-3]. On the other hand, the smaller, euhedral dolomites (Fig. 1f) lack dislocations and were found in contact with large, anhedral apatites and dolomites. These observations indicate that the Ryugu samples were modified by multiple dissolution and precipitation events, and some of these events occurred after the shock processes, potentially as a result of the shock processes, as described by [10]. No space-weathering effects were observed in any dolomite or apatite crystals.

Our TEM observations demonstrate variability in the shock metamorphic effects among carbonates, indicating that not all carbonates were affected by the mild shock metamorphism described in previous studies [4]. Notably, the large dolomite crystal was the most significantly impacted by shock metamorphism. However, the absence of these shock features in certain

carbonate crystals implies their formation through multiple growth episodes facilitated by dissolution/precipitation processes. This suggests that some dolomites may have predated the formation of certain calcite crystals, a hypothesis that may be supported by distinct oxygen isotopic signatures among different calcite crystals [7].

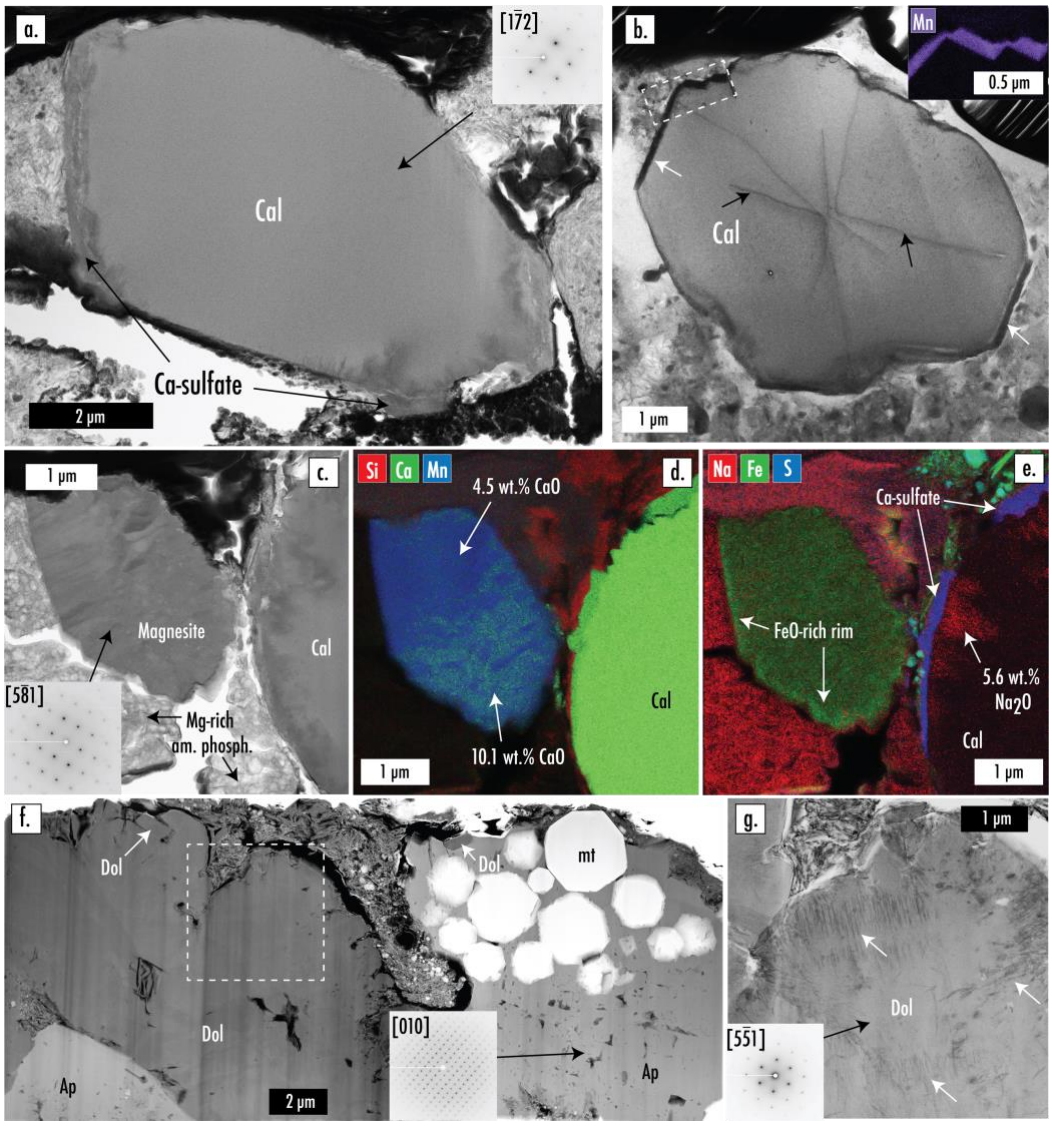

Figure 1. a) Nanobeam diffraction (NBD) image of calcite (Cal, [1-72] zone axis) showing no defects or space weathering effects. This calcite exhibits an overgrowth of calcium sulfates. b) NBD image of calcite from FIB section A0104-026087, revealing radial dislocations (black arrows) and a Mn-rich, heterogeneous euhedral rim (highlighted by white arrows and supported by the energy-dispersive X-ray spectroscopy (EDS) map, white dashed box from Fig. 1b: Mn – purple). c) NBD images of the Mn-rich magnesite associated with calcite and Mg-rich amorphous phosphate (Mg-rich am. phosph.). d-e) Composite EDS maps of Si, Ca, and Mn (d), and Na, Fe, and S (e), showing heterogeneities in calcite and the Mn-rich magnesite (from Fig. 1c). f) Dark-field scanning transmission electron microscopy (STEM) image of one of the FIB sections prepared at the boundary between the large dolomite (Dol) and apatite (Ap, [010] zone axis). Framboidal magnetite (mt) is embedded within the porous apatite. Small (~1 µm in length) euhedral dolomites are indicated by white arrows (from Fig. 1f). g) NBD image of the dolomite crystal ([5-51] zone axis, white dashed box from Fig. 1f) containing numerous defects (see white arrows) produced through shock metamorphism.

References

[1] Tyra M. et al. (2012) *Geochimica et Cosmochimica Acta*, 77:383-395. [2] Dobrică E. et al. (2024) *Geochimica et Cosmochimica Acta*, 368:112–125. [3] Dobrică E. et al. (2022) *Geochimica et Cosmochimica Acta*, 317:286-305. [4] Tomioka N. (2023) *Nature Astronomy*, 7:669-677. [5] Nakamura T. et al. (2022) *Science*, 10.1126/science.abn8671. [6] Kawasaki N. et al. (2022) *Science Advances*, 8:eade2067. [7] Fujiya W. et al. (2023) *Nature Geoscience*, 16:675-682. [8] Shih M. et al. (2021) *Nature Communications*, 12:3590. [9] Gounelle M. and Zolensky M. E. (2001) *Meteoritics & Planetary Science*, 36:1321-1329. [10] Rubin A. E. (2012) *Geochimica et Cosmochimica Acta*, 90:181-194.

Why is the asteroid Ryugu darker than CI chondrites?
- Consideration based on heating experiments of CI chondrites

Seima Ishida[1], Tomoki Nakamura[1], Megumi Matsumoto[1], Kana Amano[2], Takahiro Kawai[3], Shohei Yamashita[4] and Yoshio Takahashi[3]

[1]*Department of Earth Science, Tohoku University, Sendai 980-8578, Japan.* [2]*Institute of Mineralogy, Physics of Materials and Cosmochemistry, National Museum of Natural History, 75005 Paris, France.* [3]*Department of Earth and Planetary Science, The University of Tokyo, Tokyo 113-0033, Japan..* [4]*Photon Factory, Institute of Materials Structure Science, High-Energy Accelerator Research Organization, Tsukuba 305-0801, Japan.*

Introduction: Ryugu samples are chemically and mineralogically similar to CI chondrites[1][2]. On the other hand, there are significant differences between the reflectance spectra of Ryugu samples and CI chondrites, while those of Ryugu samples are similar to those of the CI chondrite samples heated at 300℃ under reducing conditions[3]. The previous study performed heating experiments of Orgueil CI chondrite and compared the spectrum of Orgueil heated at 150℃ for 3 hours in an N_2 atmosphere (preheated Orgueil), and those of Orgueil heated at 300℃ for 50 hours and 100 hours under reducing conditions, and those of the Ryugu samples (Fig. 1)[3]. Fig. 1 shows that the spectrum of Orgueil heated shortly at 150℃ differs significantly from those of the Ryugu samples, while those of Orgueil heated at 300℃ under reducing conditions are quite similar to those of the Ryugu samples, with becoming darker especially at the visible–near-infrared (Vis-NIR) wavelengths. The possible causes responsible for the spectral differences between the 150℃-heated Orgueil sample and the Ryugu samples are the formation of bright hydrous sulfates and/or the oxidation of Fe^{2+} to Fe^{3+} in phyllosilicate-rich matrix in Orgueil by terrestrial weathering[3]. However, it is not yet identified the cause of the spectral differences. Therefore, this study aims to understand what chemical and mineralogical changes occur in Orgueil samples during experimental heating at 300℃ under reducing conditions and to identify the actual causes of spectral differences between Orgueil and Ryugu samples. We conducted heating experiments of Orgueil samples at 100℃ and 300℃ under reducing conditions, at 100℃ and 300℃ in air (oxidizing conditions). All samples were examined using FE-SEM, FE-TEM, FT-IR, XRD, and STXM to characterize mineralogical and chemical changes by the experimental heating.

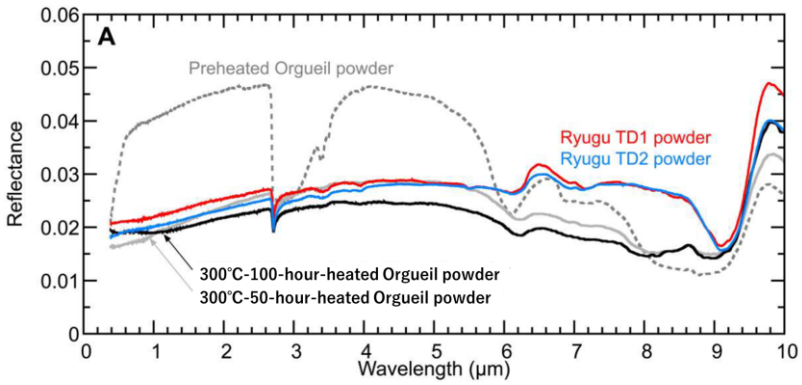

Fig. 1. Spectral comparison between Ryugu samples and Orgueil. There are reflectance spectra of powder samples of Ryugu, preheated Orgueil and 300°C-heated Orgueil under reducing conditions (Modified Fig. 5A in [3]).

Results and Discussion: Fig. 2 shows the spectra of unheated Orgueil and those of heated Orgueil. First, regarding the heating under reducing conditions (Fig. 2A), the spectra of Ryugu samples[1] were not reproduced by Orgueil heated at 100℃ under reducing conditions (Orgueil 100℃ re) but were reproduced by Orgueil heated at 300℃ under reducing conditions (Orgueil 300℃ re), and this result is consistent with the previous study[3]. Here we discuss possible causes of the spectral changes based on FE-SEM, FE-TEM, XRD, and STXM analyses. We found that the following changes occur in the Orgueil samples heated at 300℃ under reducing conditions: dehydration of sulfates, alteration of ferrihydrite, alteration of organic matter, and an increase in submicron-scale pores. Smectite, a major component of Orgueil, becomes brighter at the Vis-NIR wavelengths with an increase in submicron-scale pores[4][5]. Therefore, the increase in submicron-scale pores in Orgueil is not likely the reason why Orgueil becomes much darker by heating at 300℃ under reducing conditions. Synchrotron STXM (PF BL-19A) analysis showed that $Fe^{2+}/\Sigma Fe$ ratios of phyllosilicates in the unheated and 300℃-heated Orgueil samples are similar, suggesting that no reduction of Fe^{3+} took place during heating. This suggests that Fe valence in Orgueil phyllosilicates is not likely the cause responsible for the darkening of Orgueil spectra.

Second, regarding the heating under oxidizing conditions (Fig. 2B), the spectrum of Orgueil heated at 100℃ under oxidizing conditions (Orgueil 100℃ ox) is a little brighter than that of unheated Orgueil (Orgueil unh ox) from 0.38 to 2.7 μm in wavelength. The spectrum of Orgueil heated at 300℃ under oxidizing conditions (Orgueil 300℃ ox) becomes much brighter from 0.38 to 6.0 μm in wavelength. Currently, we cannot identify the reason why the spectra of Orgueil heated under

oxidizing conditions became brighter, but it is clear that the "masking effect" caused by dark organics and/or other dark material becomes weaker by heating under oxidizing conditions. It is known that adding a small amount of carbon black to white phyllosilicate montmorillonite results in a large darkening of the spectrum and reduction of the absorption strength at the Vis-NIR wavelengths (see also Fig. S9 in [3], originally from RELAB Spectral Database), which is called the "masking effect". The weakening of the masking effects is supported by the fact that the spectrum of Orgueil heated at 300℃ under oxidizing conditions has a deeper peak at ~2.0 μm due to phyllosilicates than that of unheated Orgueil.

We performed reheating under reducing conditions of the Orgueil samples once heated under oxidizing conditions: the Orgueil samples that had been heated at 300°C under oxidizing conditions were heated again at 300°C under reducing conditions (Orgueil 300℃ oxre). Such heating under reducing conditions darkened Orgueil spectra once again and reproduced the spectra of the Ryugu samples (Fig. 2B). We found that the brightness change is reversible and the material responsible keeps staying in Orgueil during heating and just changes the brightness by some structural or chemical changes. The above results suggest that there are originally dark materials in CI chondrites that change their brightness significantly by heating at 300°C under oxidizing and reducing conditions.

Candidates responsible are sulfates, ferrihydrite, and organic matter, but we cannot identify which is a major component for the observed spectral change. We will continue detailed observation and analysis of the heated Orgueil samples to determine which process among dehydration of sulfates, alteration of ferrihydrite, and alteration of organic matter is mainly responsible for the spectral differences between the unheated and heated Orgueil and also between the unheated Orgueil and Ryugu samples.

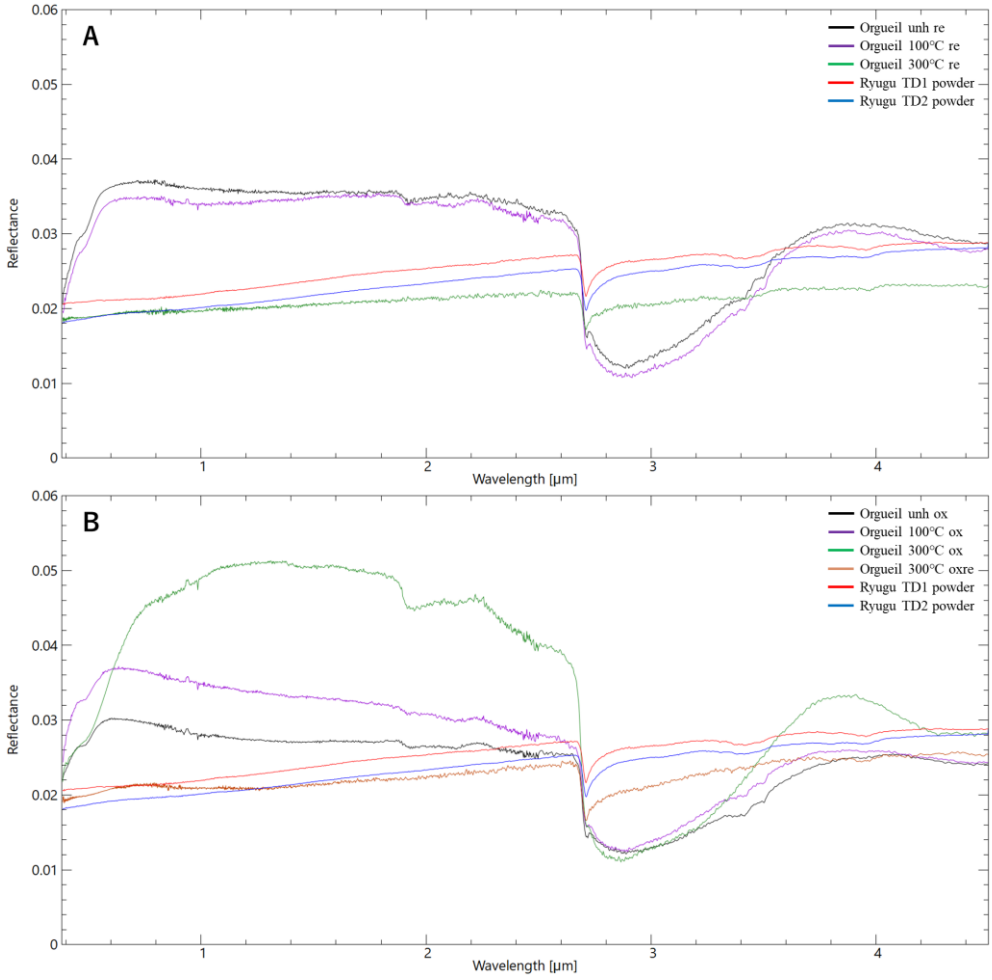

Fig. 2. (A) Reflectance spectra of the Ryugu samples, unheated Orgueil (Orgueil unh re) and Orgueil heated under reducing conditions (Orgueil 100°C re and Orgueil 300°C re). (B) Reflectance spectra of the Ryugu samples, unheated Orgueil (Orgueil unh ox), Orgueil heated under oxidizing conditions (Orgueil 100°C ox and Orgueil 300°C ox) and Orgueil reheated at 300°C under reducing conditions after the heating at 300°C under oxidizing conditions.

References

[1] Nakamura et al. (2023) Science, **379**, eabn8671. [2] Yokoyama et al. (2023) Science, **379**, eabn7850. [3] Amano et al. (2023) *Sci. Adv.* **9**, eadi3789. [4] Sultana et al. (2021) Icarus, **357**, 114141. [5] Poch et al. (2016) Icarus, **267**, 154–173.

Io Sample Return: A Critical Missing Link in Planetary Science

Ryan Ogliore
Washington University in St. Louis

Introduction: Volcanic plumes on Jupiter's moon Io launch pyroclastic debris more than 10 km above its surface, offering an opportunity for sample return from a world about the size our Moon without the cost and complexity of a landed mission [1]. With a few hundred milligrams of this material, high-precision lab isotope and element measurements of "bulk silicate Io" can tell us about Io's origin and early evolution (information that is erased from its young surface) [2]. Though Io, with its extreme tidally-driven volcanism, may seem like a Solar System oddball, it is actually a critical missing link in our understanding of the Solar System's origins, the formation and early evolution of planets, habitability in tidally heated worlds, and exoplanets.

Link between Noncarbonaceous and Carbonaceous Solar System Reservoirs: The NC and CC reservoirs are proposed to have been kept separate by an early forming Jupiter [3]. High-precision analyses of Cr, Ti, and other isotope systems can test models of these hypothetical Solar System reservoirs. If carbonaceous chondrites formed in the outer Solar System and were the building blocks of the giant planets, the isotopic composition of the Io sample could be expressed as a linear combination of known carbonaceous chondrites. An alternative, and more likely, hypothesis is that our understanding of the Solar System's building blocks is incomplete because our collections are limited to bodies currently on Earth-crossing orbits. In this scenario, the composition of the Io sample could not be expressed in terms of known meteorite types.

Link between the formation and adolescence of the terrestrial planets: Io may be a window back to the early years of Earth and the other terrestrial planets. In the heat-pipe model, Io is representative of the terrestrial planets after the magma ocean phase and before the stagnant lid [4]. High-precision measurements of Fe, Mg, and Si can give insights into high-temperature volatile depletion in a heat-piping Io. Additionally, Io may erupt very high temperature lavas that are similar to komatiites from the Archean period of the ancient Earth [5]. An understanding of the similarity of Io's lavas to Earth's lavas is only possible with high-sensitivity measurements of major, minor, and trace elements of Io's lava in Earth labs.

Link between planet formation times in the inner and outer Solar System: The formation time of Io's core, with ~0.1 Myr precision, can be calculated using the Hf-W system on a returned Io sample. This age can be compared to the formation ages of the Earth, Moon, Mars, and Vesta [6]. Once Io's formation age is known, we can use accretion models to better understand the formation times of the Jovian system and other bodies in the outer Solar System. The abundance of W in the Io sample will likely be low, ~200 ppbw, but current analytical techniques are so sensitive that we only need nanograms of W to make the measurement [7] (corresponding to less than 5% of the anticipated collected sample mass).

Link between icy builidng blocks and habitability: Io's neighbor Europa is a possibly habitable ocean world. Io may have formed icy, like Europa, and subsequently lost its volatiles. A signature of a volatile-rich origin for Io would be recorded in mass-dependent fractionation of volatile and moderately volatile elements in a collected Io sample ($^{34}S/^{32}S$ has been measured telescopically to be high in Io [8]). Currently, Io may be delivering elements necessary for life to Europa's surface through its volcanic eruptions [9]. High-sensitivity analyses of Io's volcanic material will yield the abundances and types of matter that may be deposited on Europa's surface, where it may eventually be incorporated into its subsurface ocean. Additionally, Ionian volcanic emissions can become ionized and interact with Jupiter's magnetosphere to create the Io plasma torus. This irradiation environment is inhospitable to life, unless it is shielded (e.g., by Europa's ice shell) . It is possible to understand the formation mechanism of the Io plasma torus through combined analyses of returned ions, dust, and gas from Io.

Link between the Solar System and exoplanetary systems: Ganymede, Europa, and Io are locked in a 4:2:1 orbital resonance, similar to some exoplanetary systems [10]. Tidal heating can be a major cause of geologic evolution in exoplanets, as it is on Io. A possible exo-Io, detected by a Na cloud, has been discovered around a hot Saturn orbiting the Sun-like star WASP-49 [11]. Understanding Io's building blocks, formation age, and volatile loss will help us understand how tidally heated exoplanets elsewhere formed and evolved.

References: [1] Davis, A. B., et al. (2024) IEEE Aerospace Conference. [2] Ogliore, R. C., et al. (2023), LPSC, Abstract #1326. [3] Kruijer, T. A., et al. (2017) PNAS 114(26), 6712. [4] Moore, W. B., et al. (2017) EPSL 474, 13. [5] Williams, D. A., et al. (2000) JGR:P 105(E1), 1671. [6] Kleine, T. & Walker R. J. (2017) Annu. Rev. Earth Planet. Sci**.** 45, 389. [7] Zhang, T., et al. (2023) Geostand. Geoanal. Res. 47(1), 169. [8] de Kleer, K., et al. (2024) Science 384(6696), 682l [9] Becker, T. M., et al. (2022) PSJ 3(6), 129. [10] Leleu, A. et al. (2021) A&A 649, A26. [11] Oza, A. et al. (2024) ApJL *in press*.

Thermophysical Properties of Aseroid Bolders in Hayabusa2, Hera, and Future Missions

Tatsuaki Okada[1,2], Satoshi Tanaka[1,2], Naoya Sakatani[1], Yuri Shimaki[1], Takuya Ishizaki[1], Takehiko Arai[3], Hiroki Senshu[4], Hirohide Demura[5], Tomohiko Sekiguchi[6], Toru Kouyama[7], Masanori Kanamaru[2], and TIRI Team[1]

[1]*ISAS, Japan Aerospace Exploration Agency,* [2]*University of Tokyo,* [3]*Maebashi Institute of Technology,* [4]*Chiba Institute of Technology,* [5]*University of Aizu,* [6]*Hokkaido University of Education,* [7]*AIST*

Thermal imaging is a powerful tool to investigate thermophysical properties indicate physical state of materials such as porosity, grain size, and crystallinity, and also compositional information if spectral information is obtained. Thermal imaging of C-type asteroid Ryugu has been conducted in JAXA Hayabusa2 mission using a thermal imager TIR [1], which successfully imaged the entire surface of an asteroid for the first time, to study the surface thermal inertia, especially the surface boulders. We found most of boulders has lower thermal inerita of 200-400 J kg^{-1} m^{-2} $s^{-0.5}$ (tiu, hereafter) than that of typical carbonaceous chondrites [2]. On the other hand, the thermal diffusivity measurements of returned sample from Ryugu indicate that the samples show the thermal inertia almost the same as typical carbonaceous chondrites of ~1000 tiu, but much lower value in the direction where cracks exist [3]. It seems likely that the materials on Ryugu originally is basically a typical chondrite-like material but with more cracks and pores. TIR will observe the other S-type asteroid Torifune (2001 CC21) during its flyby in 2026, and unknown type (probably L- or D-type) small asteroid 1998 KY26.

In ESA Hera mission, which is going to be launched in Oct 2024, a thermal infrared imager TIRI [4] is developed to investigate thermophysical properties and conposition of the constituent materials of surface boulders of S-type asteroid Didymos and Dimorphos. TIRI is capable of thermographoc imaging using a mid infrared wide band and of compositional imaging using six narrow bands. TIRI will inform thermophysical properties and composition of Didymos, which has the rough surface and a relatively smoother equatorial region, as well as those of Dimorphos, which is entirely covered with boulders. In this mission, the surface properties will be also measured by small CubeSats and the results will be compared between multiple measurements. The instrument will be possibly used for ESA-led RAMSES mission to investigate the S-type Earth-approaching asteroid Apophis.

In the next generation small body sample return (NGSR) mission under study in Japan, a similar but probably improved thermal imager will be developed to investigate a comet (currently the target is 289P/Branpain) with a wide band therma imaging and multi-bands compositional imaging. We present here the instrumentation and concept of operation in Hayabusa2, Hera, Ramses, and the future missions.

References

[1] Okada. T. et al. 2017. Space Sci. Rev. 208, 255-286. [2] Okda, T. et al. Nature 579, 518-522. [3] Ishizaki T. et al., 2023, Intl. J. Thermophys. 43, 51., [4] Okada, T. et al., Space Sci, Rev., *in prep.*

The Next Generation small-body Sample Return mission: a concept study of a comet sample return

Yuri Shimaki[1], Hiroyuki Kurokawa[2], Naoya Sakatani[1], Ryota Fukai[1], Tatsuaki Okada[1], Jun Aoki[3], Yoko Kebukawa[4], Atsushi Kumamoto[5], Satoshi Tanaka[1], Taichi Kawamura[6], Hiroki Senshu[7], Ryo Suetsugu[8], Seitaro Urakawa[9], Eri Tatsumi[1], Yuki Takao[10], Shota Kikuchi[11], Osamu Mori[1], Takanao Saiki[1], and Yuichi Tsuda[1]

[1]*Japan Aerospace Exploration Agency,* [2]*University of Tokyo,* [3]*Osaka University,* [4]*Tokyo Institute of Technology,* [5]*Tohoku University,* [6]*Université Paris Cité/Institut de Physique du Globe de Paris, CNRS,* [7]*Chiba Institute of Technology,* [8]*Oshima National College of Maritime Technology,* [9]*Japan Spaceguard Association,* [10]*Kyusyu University,* [11]*National Astronomical Observatory of Japan*

The Next Generation small-body Sample Return (NGSR) mission is a small-body sample return mission following Hayabusa2 and MMX, as a candidate for JAXA/ISAS's strategic large-class mission to be realized in the 2030s. The main goal of NGSR is to develop an innovative deep space round-trip exploration system consisting of a Deep Space Orbital Transfer Vehicle (DSOTV) and a separative touch-and-go sampling probe and to realize samples return from a primitive small body for elucidating the origins of the solar system and life in the Galaxy.

Considering the results and issues of Hayabusa2, we have set the scientific goals as (SMG-I) to elucidate the origin of solar system "materials" by tracing the evolution of galactic materials and (SMG-II) to elucidate the origin of solar system "objects" by approaching the process of planetesimal formation. We have selected the Jupiter-family comet 289P/Blanpain as the nominal target body. The nominal mission timeline is to launch in 2034, arrive in 2040, and return to Earth in 2046. We have multiple backup launch windows and backup objects, although the best windows are in the early 2030s for 289P.

During the proximity phase, optical navigation cameras will observe the target surface topography and determine its shape. Gravity measurements will be performed using LIDAR to estimate the bulk density of the body. Surface physical properties will be investigated using a thermal infrared imager. Combining this information, landing candidate sites will be selected. Cometary samples will be collected by touchdown operations using the probe's sampler, and volatile and organic matter will be analyzed using a small mass spectrometer. A small carry-on impactor (SCI) will be used to collect subsurface material unaffected by cometary activity, space weathering, etc. After freeze-drying the samples and rendezvous-docking the probe to the DSOTV, the samples will be transported to the small, lightweight sample return capsule on the DSOTV, then returned to Earth via ultra-high-speed reentry and hard landing (SMG-I). In addition, seismometer operations combined with the SCI/sampling operations and radar tomography observation using a multi-spacecraft system will be performed to investigate the internal structure of the cometary nucleus (SMG-II).

This presentation will introduce an overview of the mission based on the mission proposal to JAXA/ISAS and the science community in July 2024.

Could Some of the Existing Asteroid Taxonomic Classes be Explained as Space Weathered Samples of Other Classes?

Beth Ellen Clark[1], **Xiao-Duan Zou[2]**, John Brucato[3], Teresa Fornaro[3], Giovanni Poggiali[3]
[1]*Ithaca College*
[2]*Planetary Science Institute (zouxd@psi.edu)*
[3]*Laboratory of Astrobiology, INAF Arcetri Astrophysical Observatory Firenze*

Asteroids are remnants of the early Solar System formation, representing relics from the era when dust and ice accreted into planetesimals. These small bodies then coalesced to form the planets, with asteroids remaining as the vestiges of this process. Most solid matter in the Solar System was swept into planets, leaving asteroids as passive witnesses of these formative events. However, space weathering, which alters asteroid surface properties and colors over time, complicates our interpretation of the Solar System's history. Current taxonomies, which are not based on intrinsic properties such as mineralogical composition, geological history, and Earth-based meteorite analogs, but on extrinsic properties like spectral slope and band position, may be influenced by surface-altering processes. Therefore, we conducted an investigation into the robustness of asteroid taxonomy, given that even low albedo asteroids respond to space weathering by changing color.

Two recent spacecraft missions to asteroids have detected this color-changing in progress: NASA's OSIRIS-REx mission to asteroid (101955) Bennu and the Japanese Aerospace Exploration Agency's (JAXA's) Hayabusa2 mission to asteroid (162173) Ryugu. Both Bennu and Ryugu are primitive, organic- and volatile- rich assemblages of minerals that preserve material from the earliest phases of planet formation in our Solar System. We need to understand if they are "cloaking" themselves (or disguising themselves), and causing confusion as we develop our understanding of the asteroid population as a record of Solar System formation.

To investigate this, we analyzed color changes across multiple wavelengths (visible and infrared) to capture the full range of space-weathering effects on asteroid surfaces. These asteroids serve as ideal candidates due to their known organic-rich compositions and the availability of direct observational and sample data. We then use this information to study how asteroid color changes with age might explain some of the known color variation between asteroids in our Solar System and how this would impact the compositional mass distribution of the asteroid regions of the Solar System.
Currently, most known asteroids fall into either the S-complex (composed of S, Sa, Sq, Sr and Sv-types) or the C-complex (composed of C, B, Cb, Cg, Cgh, Ch, and sometimes P and D-types in the Bus-DeMeo taxonomy[1]). However, this classification primarily relies on spectral data from the surface's topmost millimeter. If the subsurface composition of an asteroid differs spectrally from the surface, this could significantly alter our interpretation of remote sensing data and our understanding of asteroid compositions. Now that we know how dark asteroid spectral properties change through time, can some of the existing taxonomic classes be explained simply as space weathered samples of other taxonomies? Here we report our efforts to understand the consequences of space weathering, a test of taxonomy robustness and implications for the compositional mass distribution of the asteroids.

References

[1] DeMeo, F.E. and Carry, B., 2013. The taxonomic distribution of asteroids from multi-filter all-sky photometric surveys. *Icarus*, *226*(1), pp.723-741.

Exploring the diversity of near-Earth asteroids: what's next?

Perna D.[1]
[1]*INAF – Rome Observatory (Italy)*

The study of near-Earth asteroids (NEAs) has revealed a great diversity in their physical properties, partly mirroring the wide variety observed in the asteroid population of the main belt. This diversity appears to contrast with a more limited range of compositions evident from meteorite collections, suggesting that meteorites may not fully represent the broader spectrum of asteroid properties. In this context, future space missions should prioritize the exploration of asteroids with different physical characteristics, especially in terms of internal structure and taxonomic type. This will offer new insights into the early stages of planetary formation and the processes governing the evolution of small bodies in the solar system.

Several upcoming missions are set to broaden our understanding of NEAs by focusing on a diverse range of targets. These include the Hayabusa2# extended mission and the OSIRIS-APEX follow-up of OSIRIS-Rex, as well as the planned missions Ramses, Tianwen-2 and Destiny+. Furthermore, CubeSat missions in deep space can represent a cost-effective and agile approach to maximize the number of asteroid visits, enabling us to explore these diverse bodies at an unprecedented scale.

In this contribution, I will present preliminary results from spectroscopic and photometric ground-based observations of asteroids Torifune and 1998 KY26, the next targets of Hayabusa2#. Additionally, I will discuss the role of upcoming CubeSat missions in targeting NEAs with distinct properties, addressing the need to explore a wider range of asteroids to refine our models of solar system formation and evolution, and to improve our understanding of the links between meteorites and their parent bodies.

Ground-based characterization of (98943) 2001 CC_{21}, the target of Hayabusa2# space mission

Marcel M. Popescu[1], Eri Tatsumi[2], Javier Licandro[3], Miguel R. Alarcon[3], Javier Rodriguez Rodriguez[4], Miquel Serra-Ricart[5], Julia de Leon[7], Joaquin Fernandez Martin[5], David Morate[6], Gabriel N. Simion[7], Bogdan Alexandru Dumitru[8], Daniel Nicolae Bertesteanu[11], George Pantelimon Prodan[1], Masatoshi Hirabayashi[10]

[1]*University of Craiova, Str. A. I. Cuza nr. 13, 200585 Craiova, Romania;* [2]*Institute of Space and Astronautical Science (ISAS),Japan Aerospace Exploration Agency (JAXA), Sagamihara,; Kanagawa, Japan;* [3]*Instituto de Astrofisica de Canarias (IAC), C/Via Lactea s/n, 38205 La Laguna, Tenerife, Spain;* [4]*Instituto Universitario de Ciencias y Tecnologias Espaciales de; Asturias (ICTEA), University of Oviedo, C. Independencia 13, E-33004 Oviedo, Spain;* [5]*Light Bridges S. L., Observatorio del Teide, Carretera del Observatorio S/N, E-38500 Guimar, Tenerife, Canarias, Spain;* [6]*Centro de Estudios de Fisica del Cosmos de Aragon (CEFCA), Unidad Asociada al CSIC, Plaza San Juan 1, 44001, Spain;* [7]*Astronomical Institute of the; Romanian Academy, 5 Cuțitul de Argint, 040557 Bucharest, Romania;* [8]*Institute of Space Science (ISS) 409, Atomistilor Street, 077125 Magurele, Ilfov, Romania;* [9]*Astroclubul Bucuresti Blvd Lascar Catargiu 21, 10663 Bucharest, Romania;* [10]*Georgia Institute of Technology, Atlanta, GA 30320, United States*

The near-Earth asteroid (98943) 2001 CC21 is the target of the Hayabusa2 extended mission (Hayabusa2#). Ground-based telescope observations play an important role in providing key scientific data for this mission. A detailed study of the asteroid was conducted between 2022 and 2024. During this time frame it reached an apparent magnitude as bright as 16.5. We determined its rotation period to be P = 5.021516 ± 0.000106 hours and its absolute magnitude H = 18.693 ± 0.10. Based on these values, we estimated its diameter to be D = 0.523 ± 0.20 km. The asteroid was classified as an Sq-type in the Bus-DeMeo taxonomy using a high signal-to-noise ratio spectrum, covering both the visible and near-infrared regions. Its mineral composition is likely similar to LL/L ordinary chondrites, with an olivine-to-pyroxene ratio (ol/(ol+px)) of 0.60, a fayalite (Fa) content of 28.5 mol%, and a ferrosilite (Fs) content of 23.4 mol%. Simultaneous observations in the g, r, i, and zs broadband filters revealed no significant large-scale heterogeneity on the surface of 2001 CC21. The extensive lightcurve data allowed us to estimate the asteroid's convex shape and pole orientation as $\lambda = 301° \pm 35°$, $\beta = 89°$ (+1°/−6°), and an axial tilt (obliquity) of $\epsilon = 5° \pm 3°$.

References

[1] Popescu, Tatsumi et al. 2024, PSJ under review

Asteroidal Treasure Hunt: Probing Prebiotic precursors in C-Type Asteroids

Olga Prieto-Ballesteros[1], César Menor-Salvan[2], Laura J. Bonales[3], Yuichiro Cho[4], Andoni G. Moral[5], Javier Sánchez-España[1], Carlos Pérez Canora[5], Iñaki Yusta Arnal[6], Andrey M. Ilin[6], Oscar Ercilla[1], Ana de Dios-Cubillas[1]

[1]*Centro de Astrobiología-CSIC-INTA. Carretera de Ajalvir km. 4, Torrejón de Ardoz, Madrid, Spain, 28850*

[2]*University of Alcalá de Henares (UAH), Km. 33,600, Alcalá de Henares, Madrid, Spain, 28805*

[3]*Centro de Investigaciones Energéticas, Medioambientales y Tecnológicas (CIEMAT). Complutense 40, Madrid, Spain, 28040*

[4]*University of Tokyo (UoT), 7-3-1 Hongo, Bunkyo, Tokyo, Japan, 113-0033*

[5]*Instituto Nacional de Técnica Aeroespacial (INTA), Crta. Ajalvir Km. 4, Torrejón de Ardoz, Spain, 28850*

[6] *Dept. of Geology, University of the Basque Country (UPV/EHU), Barrio Sarriena s/n, 48940 Leioa, Spain*

We are investigating two Ryugu fragments with identification numbers of A0542 (0.5mg) and A0552 (0.7 mg), which JAXA curation assigned to our team in the 4th Ryugu sample announcement of opportunity. Our work considers two main objectives, which pay special attention to the search for the chemical cyanide group (-CN), as well as to the primordial mineralogy in which the metal complexes -CN would be present, assessing their detection using flight models (FM) of space mission instruments. More specifically we propose:

1) Unraveling the complexities of prebiotic chemical space and the significance of non-canonical molecules (i.e., those differing from nucleic acid components, such as heterocycles) and prebiotic precursors in the formation of life's fundamental building blocks throughout the Universe. Currently, one of the major questions in origins-of-life research is the origin of nucleotides. Experimental investigations into abiotic non-canonical nucleotide synthesis revealed that many non-canonical pyrimidines and other bases, so as their related glycosides, are formed much more easily than the canonical nucleotides [1, 2, 3, 4]. Subsequently they can serve as monomers for the informational polymers by early life on Earth. These hypothetical ancestral non-canonical bases can be formed in asteroids and preserved up until now.

2) Establishing the compositional link between C- and D-type asteroids and the Martian Moons to contribute to the interpretation of data from forthcoming exploration missions. Yabuta et al. (2023) [5] showed that some organic materials are strongly associated with the mineral matrix. The matrix is mainly composed by phyllosilicates and carbonates, which have been formed by hydrothermal alteration at low temperature on the asteroid parent body. The interaction between the rock and water trigger some reactions (e.g. hydrolysis, oxidation, and aromatization) and diversity of primordial macromolecular species. Recently, some studies on the smectites (a type of layered phyllosilicate) have concluded that N-rich organics, responsible for the near infrared signature detected in Ryugu and likely detected in Ceres samples (proposed as a D-type asteroid related body, [6]), come from molecules located within the interlayer spaces of these phyllosilicates. These organic compounds can then be protected from subsequent alteration and delivered to rocky planets over the course of the Solar System's history [7]. On the other hand, this structural feature affects the Raman measurements [8, 9], and should be considered in the future observations by the RAman spectrometer for the MMX (Martian Moons eXplorer) mission (RAX) to Phobos. Results from this investigation will help to be prepared for the identification by in situ planetary Raman measurements.

We are implementing a comprehensive analytical approach to study the fragments, involving Raman spectroscopy, along with high-resolution mass spectrometry for organic molecule identification, and electron microscopy-based techniques (SEM/TEM-EDX). In addition to standard laboratory microanalysis, we are investigating these samples with flight-like models of various Raman instruments, such as RLS@Rosalind Franklin Flight Spare lab model (Fig. 1) to compare with those that might be detected during a space mission.

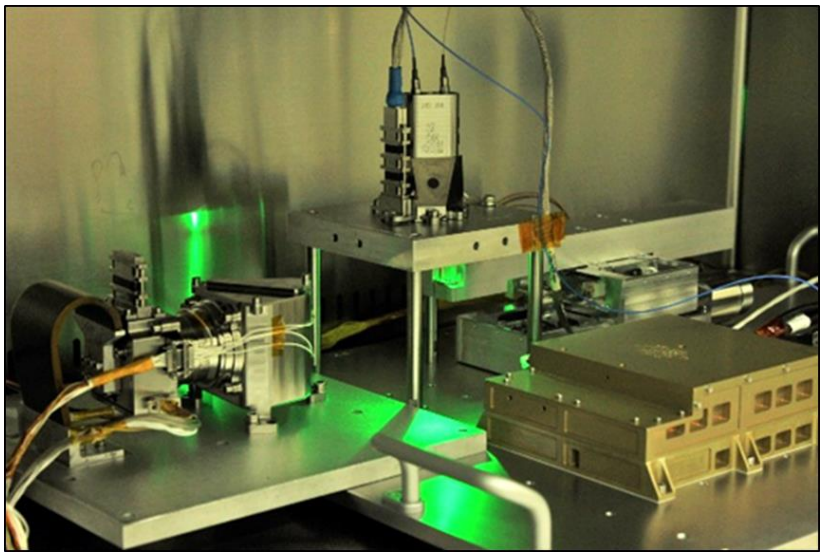

Figure 1. Picture of the Raman Laser Spectrometer for the Rosalind Franklin rover Fight Spare (RLS-FS)

We will present in the conference session the preliminary results of our study. Currently, we have already detected by electron microscopy minerals that have been commonly found in other Ryugu fragments, including fine-grained phyllosilicates (mostly serpentine and saponite-like smectites), carbonates (dolomite, Mg-rich calcite), sulfides (pyrrhotite with characteristic hexagonal platy crystals or sub-spherical aggregates, along with minor pentlandite), oxides (magnetite, commonly appearing as sub-spherical particles and coalescing in framboidal aggregates), and some other minor to accessory minerals such as hydroxyapatite, and carbonaceous fragments of still unknown composition. In agreement with previous studies, we detected neither ferrihydrite nor gypsum, which seems to be a differentiating aspect of Ryugu samples with respect to CI chondrites [11]. Chemical mapping and punctual EDX analyses of different grains and mineral aggregates have already revealed the locally abundant presence of carbon, nitrogen and phosphorus in our Ryugu samples. Further efforts in SEM-EDX and TEM studies will be focused on the detection of organics associated to the phyllosilicates (e.g., saponites) and other minerals.

We also performed some preliminary Raman tests with reference samples to determine measurement protocols to be used with the RLS-FS. We synthetized HCN-polymers and tholins to evaluate the features of disordered graphite and sp2 bonded carbon layers with N defect, which are very sensitive to laser radiation. We are building a library of cyanide complexes using ferrocyanide salts and nitriles that can be used as reference for CN Raman Bands (1900-2500 cm^{-1} area) and laser energy limits (Fig. 2). Considering that olivine and primary phosphate can be modified by cyanide and prebiotic organics in aqueous media [12], we also tested the spectral features of the formation of magnesium, calcium and ammonium ferrocyanides and Prussian blue related complexes. In addition to the synthetic samples, we tested analytical protocols to search for the -CN bands in some meteorites such as Aguas Zarcas, Kolang or NWA 14792.

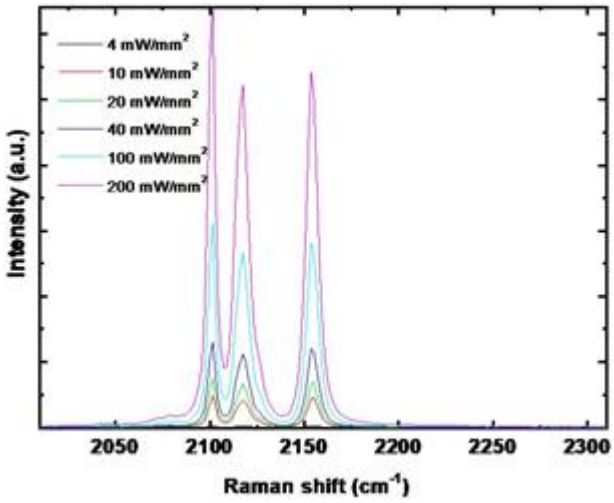

Figure 2. Raman spectra of ferrocyanicde salts and nitriles at different irradiance

References

[1] Chen, et al. (2014). Journal of the American Chemical Society, 136(15), 5640–5646. https://doi.or/10.1021/ja410124v

[2] Cafferty, et al. (2016). Nature Communications 7, 1–8. https://doi.org/10.1038/ncomms11328

[3] Fialho et al. (2020). Chemical Rev. 2020, 120, 11, 4806 – 4830. https://doi.org/10.1021/acs.chemrev.0c00069

[4] Menor Salván, et al. (2020). ChemBioChem, 21(24), 3504–3510. https://doi.org/10.1002/cbic.202000510

[5] Yabuta et al. (2023). Science 379, 6634, https://doi.org/10.1126/science.abn9057

[6] McSween et al. (2018). Meteoritics & Planetary Science 53 (9), 1793–1804. https://doi.org/10.1111/maps.12947

[7] Potiszil et al. (2020). Nature Communications 14, 1482, https://doi.org/10.1038/s41467-023-37107-6

[8] Bonal et al. (2022). EPSC Abstracts Vol. 16, EPSC2022-1131. https://doi.org/10.5194/epsc2022-1131

[9] Montagnac et al. (2021). Applied Clay Science 200, 105824. https://doi.org/10.1016/j.clay.2020.105824

[10] Astromaterials Science Research Group, Institut d'Astrophysique Spatiale, Université Paris-Saclay, CNES, Yumoto, K., Yabe, Y., Cho, Y., Sugita, S., 2022. Hayabusa2, Ryugu Sample Curatorial Dataset. https://doi.org/10.17597/ISAS.DARTS/CUR-Ryugu-description

[11] Ito, M. et al. (2022) Nature Astronomy, 6, 1163–1171, https://www.nature.com/articles/s41550-022-01745-5#Sec15

[12] Hirawaka et al (2021). Earth, Planets, and Space 73, 16. https://doi.org/10.1186/s40623-020-01352-6

Small body missions: report on the ESA Hera mission launch and ESA RAMSES

Patrick Michel
Université Côte d'Azur, Observatoire de la Côte d'Azur, CNRS, Lagrange Laboratory, Nice, France

The Hera mission, which belongs to the Space Safety Program of the European Space Agency (ESA), is the European contribution to the planetary defense Asteroid Impact & Deflection Assessment (AIDA) international cooperation. AIDA supports the development, operations and data interpretation of Hera as well as the DART mission by NASA that performed successfully the first asteroid deflection test using the kinetic impactor technique. The target of this first test is Dimorphos, the small moon of the binary asteroid (65803) Didymos. On September 26, 2022, the 580 kg DART spacecraft impacted the 151 m diameter Dimorphos at 6.1 km/s, which resulted in the reduction of the original 11h 55m orbital period of Dimorphos around Didymos by 33 minutes.

On October 7, 2024, Hera was launched successfully from Cape Canaveral on a SpaceX Falcon 9 rocket. A few days after launch, the Asteroid Framing Cameras (AFC), the Hyperspectral Imager (HyperScout-H), and the Thermal Infrared Imager (TIRI) were activated and took pictures of the Earth-Moon system, confirming their performance in the space environment. A functional checkout of the two CubeSats, Milani and Juventas, together with their payloads, was also performed successfully. A few burns in deep space lined the spacecraft up for the gravity assist at Mars in March 2025. After a fly-by of Mars and Deimos in mid-March 2025 and further deep space maneuvers, Hera will reach the Didymos system in October 2026, with close proximity operations starting in December 2026. The status, goals and measurements of Hera will be presented.

Following the success of the development of Hera in only 4 years, the European Space Agency got the authorization of pre-funding to start the development of the RAMSES mission (Rapid Apophis Mission for SpacE Safety) to the asteroid Apophis before a formal approval at the ESA Council at Ministerial Level of 2025. Apophis will perform a close approach at a distance of 32,000 km to the Earth on Friday April 13, 2029. Such a close approach for an asteroid of 340 meters in diameter is estimated to occur only once in a few millennia, which makes this event a unique opportunity for us to investigate its potential consequences on the asteroid's physical properties. We thus have the unique opportunity to observe the action of nature, through the tidal forces of the Earth that will be effective during the passage of Apophis at its closest distance to our planet. Because of its close proximity to Earth, its light will be visible to the naked eye by more than 2 billion people in the night sky on April 13, 2029 in Europe, Africa, and parts of Asia, making this event something to remember collectively. RAMSES must launch in April 2028 to reach Apophis two months before its closest approach to the Earth and characterize its properties before, during and after the approach, paving the way to the NASA OSIRIS-APEX mission that will visit Apophis a few weeks after its closest approach to the Earth for 11 months (DellaGiustina et al., 2023). The RAMSES spacecraft will be based on Hera, as due to the short timescale to develop the mission, the chosen approach is to base the mission on a re-built and adaptation of the Hera platform as well as the team structure, with some adjustment because some payloads are expected to be different. Since the development scheme and organisational structure used for Hera demonstrated its ability to develop a space mission in a rapid manner, it is thus natural to use the same approach for an even more rapid development, this time not starting from scratch. Such a fast development is in line with the necessity of being able to develop fast reconnaissance missions in the framework of planetary defense.